Development of a more energy efficient Roberts evaporator based on CFD modelling

by

Steve Pennisi

November 2004

for the degree of Doctor of Philosophy

in the School of Engineering

James Cook University

Statement of Access

I, the undersigned, the author of this thesis, understand that James Cook University will make it available for use within the University Library and, via the Australian Digital Theses network, for use elsewhere.

I understand that, as an unpublished work, a thesis has significant protection under the Copyright Act and I wish this work to be embargoed until Dec 2006.

Signature

Date

Abstract

The evaporator station within a sugar mill is the single largest consumer of low pressure steam for heating purposes. Factories have identified the need to reduce the energy requirements of the evaporator station so that larger quantities of energy can be used for co-generation and other purposes.

The design of evaporator vessels has remained unchanged since the 1950s and most alterations and design improvements made during the time since have lacked the insight afforded by such tools as CFD modelling. CFD model predictions allow for an understanding of the fluid flow behaviour which is occurring inside the vessel and can not the visualised by any other means. The ability to visualise the behaviour of the entire flow field has been identified as the possible starting point for a novel design of evaporator and significant improvements in performance.

As a result of this investigation a large number of data was gathered from factory vessels for comparison with CFD model predictions. There data did not previously exist in the literature in any suitable form. The factory data was used as part of the process to develop a CFD model capable of accurately predicting the fluid flow behaviour inside an evaporator vessel.

The subsequent application of the CFD model concluded that the existing design of evaporator vessels contained significant deficiencies in the fluid flow behaviour and that incremental changes to geometry are not likely to produce significant improvements in performance. A novel design of evaporator is presented that has been developed using the CFD model predictions. The novel design significantly improves the fluid flow behaviour inside the vessel and a greater than 30% improvement in heat transfer performance is predicted.

Despite the success of the CFD modelling included in this study, a number of areas for further investigation have been identified. These include improvements to the experimental procedure used to gather the factory data, improvements to be made to the CFD modelling tools developed to date and practical issues associated with implementation of the novel evaporator design.

Acknowledgements

The author wishes to thank the following people and organisations for their valuable contributions:

Dr Jong-Leng Liow whose knowledge in the field of fluid dynamics has been invaluable to me.

Dr Ross Broadfoot for going above and beyond the call of duty. The advice you gave was so much more than just standard supervision.

Dr Philip Schneider for assistance of all things experimental.

Dr Darrin Stephens for his knowledge of numerical modelling and for the long discussions we had.

Mr Craig Muddle for his assistance and his tireless efforts when we were conducting the factory experiments.

Sergeant Mark Retallick for all the time we spent drinking coffee, talking garbage and generally letting go of life's stresses. Duty First.

The Sugar Research Institute (SRI) for their financial support to the project and for allowing me the opportunity to complete this project.

The Australian Research Council (ARC) for their financial support.

The Queensland Government Department of State Development (QDSD) for their financial contribution.

Electronic copy

I, the undersigned, the author of this work, declare that the electronic copy of this thesis provided to the James Cook University Library is an accurate copy of the print thesis submitted, within the limits of the technology available.

Signature

Date

Statement of Sources

I declare that this thesis is my own work and has not been submitted in any form for another degree or diploma at any university or other institution of tertiary education. Information derived from the published or unpublished work of others has been acknowledged in the text and a list of references is given. I would like to acknowledge the contributions of Dr Jong-Leng Liow and Dr Philip Schneider to the accompanying co-authored paper.

Signature

Date

Contents

List of figures

List of tables

Nomenclature

A Heating surface area of an evaporator vessel (m^2)

A_o Open area ratio of the tube-plate

B Brix (%)

B_{in} Juice brix at the inlet of the vessel (%)

B_{out} Juice brix at the outlet of the vessel (%)

Cp_l Specific heat capacity of the liquid phase ($J \cdot kg^{-1} \cdot K^{-1}$)

C_{sf} Surface-fluid constant used in the Rohsenow (1952) equation for heat transfer

$C_{\varepsilon 1}$ Constant used in the $k-\varepsilon$ turbulence model (1.44)

$C_{\varepsilon 2}$ Constant used in the $k-\varepsilon$ turbulence model (1.92)

DS Dry substance by mass (%)

HTR Heat transfer ratio

$\frac{I}{W}$ Ratio of impurities to water concentration by mass

Ja Dimensionless Jacob Number, defined as: $\frac{Cp(T_s - T_{sat})}{h_{fg}}$

K Von Karman constant (0.417)

P Purity (%)

P_k Turbulence production due to viscous and buoyancy forces, used in the $k-\varepsilon$ turbulence model ($kg \cdot m^{-1} \cdot s^{-3}$)

Pr Dimensionless Prandtl Number, defined as: $\frac{Cp\mu_l}{\kappa_l}$

Q	Total heat flow through the calandria (W)
Q_e	Heat flow through the calandria causing evaporation (W)
Q_c	Heat flow through the calandria as a result of condensation (W)
Q_s	Heat flow through the calandria causing sensible heating of the liquid phase (W)
Re	Reynold's number
$\frac{S}{W}$	Ratio of sucrose to water concentration by mass
S_C	Additional mass source term in the continuity equations ($kg \cdot m^{-}1 \cdot s^{-1}$)
S_E	Additional energy source term in the energy equations ($J \cdot m^{-3} \cdot s^{-1}$)
S_M	Additional momentum source term in the momentum equations ($kg \cdot m^{-2} \cdot s^{-2}$)
T	General fluid temperature (K)
T_e'	Boiling point elevation temperature (BPET) at atmospheric pressure (K)
T_e	Boiling point elevation temperature (BPET) at a given pressure (K)
T_o	Juice temperature at the outlet of the vessel (^oC)
T_s	Saturation temperature of water at pressure under consideration (K)
U	Vessel average heat transfer coefficient (HTC) ($W \cdot m^{-2} \cdot K^{-1}$)
U_t	Typical Australian vessel average heat transfer coefficient (HTC) ($W \cdot m^{-2} \cdot K^{-1}$)
V	Velocity vector for general fluid ($m \cdot s^{-1}$)
$\bar{V}$	Average component of velocity in turbulent flow ($m \cdot s^{-1}$)
V'	Fluctuating component of velocity in turbulent flow ($m \cdot s^{-1}$)

V^+ Dimensionless near wall velocity

V_g Velocity vector for the gas phase ($m \cdot s^{-1}$)

V_l Velocity vector for the liquid phase ($m \cdot s^{-1}$)

W_g Mass flow rate of vapour ($kg \cdot s^{-1}$)

W_l Mass flow rate of liquid ($kg \cdot s^{-1}$)

X Mass fraction of vapour present in a given volume of fluid (fluid quality)

Y_g Volumetric flow rate of vapour ($m^3 \cdot s^{-1}$)

Y_l Volumetric flow rate of liquid ($m^3 \cdot s^{-1}$)

d Internal diameter of the heating tubes (m)

e Enthalpy ($kJ \cdot kg^{-1}$)

f Friction factor as applied in the Colebrook equation

g Acceleration due to gravity (9.81 $m \cdot s^{-2}$)

h_{fg} Latent heat of evaporation ($J \cdot kg^{-1}$)

h_g Enthalpy of the gas phase ($kJ \cdot kg^{-1}$)

h_l Enthalpy of the liquid phase ($kJ \cdot kg^{-1}$)

k Turbulence kinetic energy, used in the $k - \varepsilon$ turbulence model ($m^2 \cdot s^{-2}$)

k_l Kinematic diffusivity of brix in solution ($m^2 \cdot s^{-1}$)

$\dot{m}_e$ Mass flow rate of vapour produced by evaporation ($kg \cdot s^{-1}$)

$\dot{m}_c$ Mass flow rate of condensate out of the calandria ($kg \cdot s^{-1}$)

$\dot{m}_{in}$ Mass flow rate of juice at the inlet of the vessel ($kg \cdot s^{-1}$)

$\dot{m}_{out}$ Mass flow rate of juice at the outlet of the vessel ($kg \cdot s^{-1}$)

n Fluid constant used in the Rohsenow (1952) equation for heat transfer

p Pressure (Pa)

q_g Heat flow into the gas phase (W)

q_l Heat flow into the liquid phase (W)

t Time (s)

y^+ Dimensionless distance from the wall

ΔT Effective temperature difference between the heating fluid and the heated fluid (K)

α_g Volume fraction of gas phase

α_l Volume fraction of liquid phase

ε Turbulence eddy dissipation, used in the $k-\varepsilon$ turbulence model ($m^2 \cdot s^{-3}$)

φ Any specific variable in the vector equations

κ_l Thermal conductivity of the liquid phase ($W \cdot m^{-1} \cdot K^{-1}$)

μ General fluid viscosity (Pa·s)

μ_g Viscosity of the gas phase (Pa·s)

μ_l Viscosity of the liquid phase (Pa·s)

μ_m Average fluid viscosity based on fluid quality (Pa·s)

μ_t Turbulence viscosity, used in the $k-\varepsilon$ turbulence model (Pa·s)

ρ Density of general fluid ($kg \cdot m^{-3}$)

ρ_g Density of the gas phase ($kg \cdot m^{-3}$)

ρ_l Density of the liquid phase ($kg \cdot m^{-3}$)

ρ_m Average fluid density based on fluid quality ($kg \cdot m^{-3}$)

τ_w Wall shear stress (Pa)

σ_k Constant used in the $k-\varepsilon$ turbulence model (1.0)

σ_l Surface tension of the liquid phase ($N \cdot m^{-1}$)

σ_ε Constant used in the $k-\varepsilon$ turbulence model (1.3)

1. Introduction

Sugar is Australia's second largest export crop and Queensland's largest agricultural commodity. Queensland currently produces approximately 95% of Australia's raw sugar with the remainder produced in New South Wales and Western Australia. In Australia, 520,000 hectares of land are currently under cane and this area is increasing, particularly in the Burdekin, Herbert, Tully and Proserpine regions. Figure 1.1, from Queensland Sugar Corporation (2001) , gives an overview of the sugar industry regions around Australia. Australia produces raw and refined sugars both for export and internal consumption. In order to clarify the many industry specific terms, a glossary of terms is provided in Appendix A. The majority of the terms seen in Appendix A were obtained from Stephens (2001) and Bureau of Sugar Experiment Stations (BSES) (1992).

Figure 1.2 shows the manufacturing process involved in the production of raw sugar. The numbers shown on Figure 1.2 correspond to the steps detailed as follows:

1. **Growing.** Cane grown in the field is harvested using mechanical harvesters and transported to the factory on a small gauge railway system.

2. **Shredding.** The cane is weighed and dumped onto a conveyor belt and then passed through a shredder to form a coarse pulp. The shredder breaks open the fibrous cells and makes the juice more accessible to be extracted. Upon leaving the shredder the pulp is known as prepared cane.

3. **Milling.** The prepared cane is squeezed in a sequential series of grooved rolls. This process is known in the industry as milling. The juice is removed from the bottom of the mills and the fibre (bagasse) is passed to the next milling stage for further squeezing. Most factories employ four or five milling stages and use counter-current washing, with water and juice, in the mills to maximise the removal of sucrose from the cane cells.

4. **Bagasse storage.** The bagasse exiting the final milling stage is stored in stockpiles and returned to the factory's boiler station as fuel for combustion. The boiler station provides high-pressure steam for turbine drives on the shredder, mills and the turbo-alternators. Factories produce electricity for internal consumption and export small amounts of power to the state grid.

5. **Clarification.** The juice extracted from the first and second milling stages is combined and then heated with low-pressure (LP) steam from the exhaust of the turbines or vapour withdrawn from the evaporator station. Lime is added to adjust the pH to approximately 7.8 and to form a precipitate of calcium phosphate. This precipitate coagulates with mud (soil) particles to form flocs that settle out in vessels called clarifiers. The mud removed in the clarification stage is processed through rotary vacuum filters to reduce the sucrose content contained in the mud. The mud cake from the filters is returned to the fields as mill mud.

6. **Juice storage.** The clarified juice is passed to an intermediate storage termed the Evaporator Supply Juice (ESJ) tank in order to buffer out any fluctuations in the juice supply. Some factories divert small quantities of clarified juice to other parts of the factory to replace the use of water and therefore reduce the loading on the evaporator stage.

7. **Evaporation.** The ESJ is passed through a multiple effect evaporator station that generally comprises quadruple or quintuple evaporators, Wright (1983). The evaporators boil off the majority of excess water contained in the juice, without supersaturating the sucrose mixture. When referring to all of the evaporator vessels the term "evaporator set" or simply "set" is used. The first evaporation stage is at a pressure slightly above atmospheric pressure (115 kPa abs) and the final stage is under vacuum (15 kPa abs). The operating pressure of each evaporation stage in the set decreases progressively from the first to the last stage. Each evaporation stage is known as an effect, each effect can consist of a single vessel or a number of vessels running in parallel. The first effect uses LP steam, from the exhaust of the turbines, as the heating source and subsequent effects use the vapour boiled off in the previous effect as the heat source. After the final stage of evaporation the juice is called syrup or liquor.

8. **Crystallisation.** The syrup is boiled again under high vacuum (15 kPa abs) in evaporative crystallisation pans. The boiling super-saturates the syrup and seed crystals are added to the liquid to initiate crystal growth. The mixture of crystals and liquid is now called massecuite.

9. **Fugalling.** The crystals are removed from the liquid by spinning the massecuite at high speed in perforated baskets called centrifuges. The

massecuite is separated into crystals and molasses. The molasses is then recycled and boiled again to recover more of the sucrose from the solution. Australian factories predominantly use the three-massecuite formula where the molasses is re-boiled three times. The first vacuum pan is called the 'A' pan, the second stage the 'B' pan and the third stage is the 'C' pan, with the purity of the massecuite boiled decreasing after each boiling. Molasses leaving the third stage is called final molasses and is predominantly used as cattle feed or as feedstock for fermentation. The sugar crystals produced in the third stage are not sent to product but are recycled to the A and B pans as seed, or are remelted and mixed with the syrup entering the A and B pan stages.

10. **Drying.** The raw sugar crystals produced by the A and B pans are dried by tumbling through a counter-current airflow in a rotary drum. The raw sugar product is then sent to storage bins to await shipment.

11. **Co-generation.** Sugar mills produce electricity for internal consumption by passing high-pressure steam from the bagasse-fired boilers through turbo-alternators. In some cases excess electricity is produced and exported to the state grid. This process is known as co-generation.

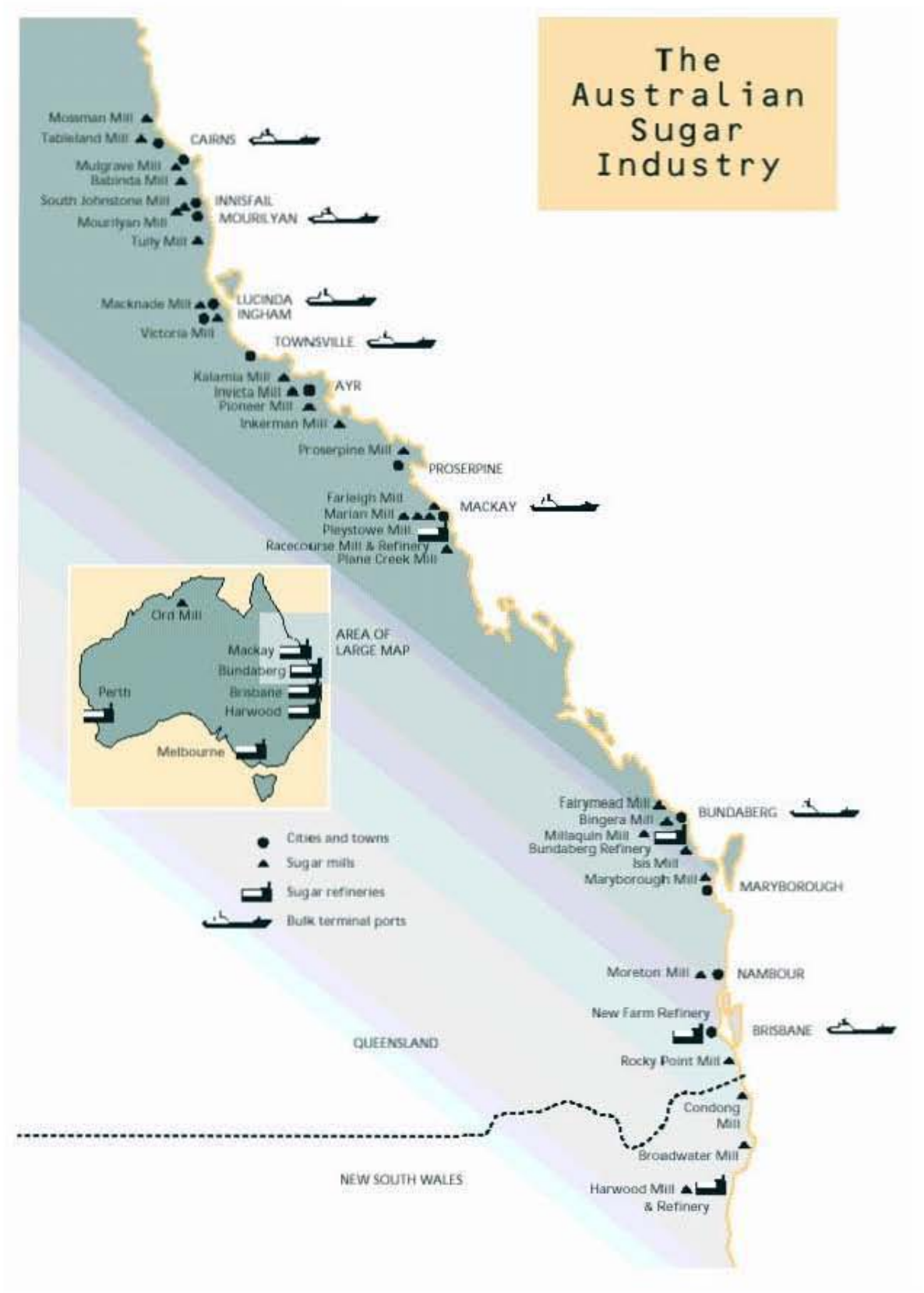

Figure 1.1 Australian sugar industry regions, Queensland Sugar Corporation (2001)

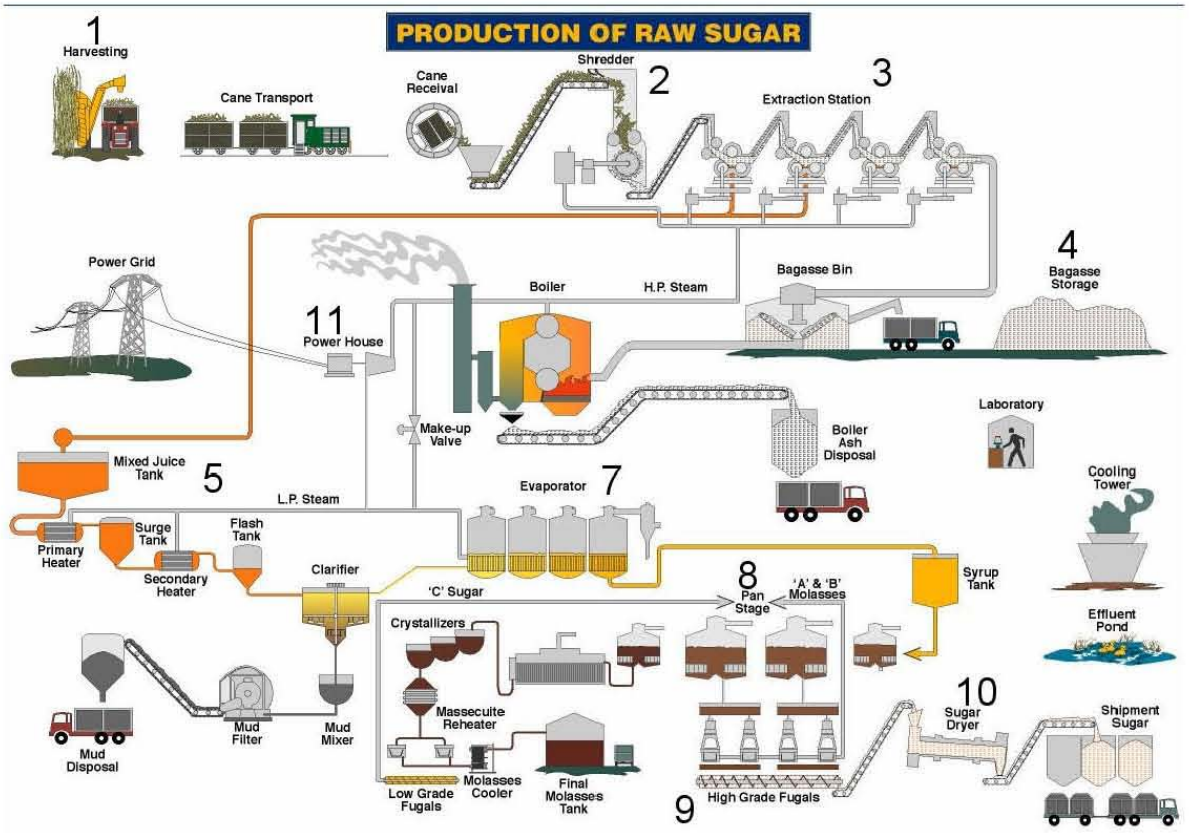

Figure 1.2 The process of raw sugar production

1.1 Types of evaporator vessels

The Australian sugar industry utilises both plate and tube type vessels. Both the plate and the tube type vessels can operate as falling film or rising film mode. The falling or rising film designation is in reference to the direction of juice flow, e.g. the juice in a rising film tube type evaporator enters the vessel beneath the heating element and rises up through the vertical heating tubes or plates, due to the boiling action of the juice inside the tubes.

1.1.1 Plate type evaporators

Plate type evaporators have a series of wafered plates packed together with the hot and the cold fluids on either side. The juice is boiled inside the plate pack and the liquid / vapour mixture passes through to the outlet. The advantages of the plate type evaporators are that they tend to be more compact than tube types, are easier to increase the heating surface area (HSA) and they tend to have higher heat transfer coefficient (HTC) and lower temperature differences than the tube type vessels. The disadvantages are that they are more expensive per unit HSA to install, are prone to increased scaling rates and for the gasketted types, are

more expensive to maintain. They also require more stringent control in order to maintain peak operational efficiency.

Rising film plate type evaporators can be used as a booster in conjunction with another tube type vessel or as a stand-alone. When operating as a booster type vessel the outlet of the plate evaporator splits into two lines. The heavier liquid is withdrawn from the bottom and piped to the juice space of a tube type vessel and the lighter vapour is piped into the vapour space of the same vessel. When operating in this configuration the plate evaporator is said to be operating as a booster since it must have pipe connections to another Roberts type vessel operating under the same process conditions. Figure 1.3, from Alfa-Laval (2001), is an open in-line for assembly picture of an Alfa-Laval plate type, rising film evaporator used to operate as a booster. Plate type evaporators can also operate as stand-alone in a configuration whereby the heating plate pack is contained within a circular vessel for the containment of the juice and vapour. Figure 1.4, from Grant *et al.* (2000), shows a plate type, falling film evaporator with the heating plates inside a vapour recovery vessel.

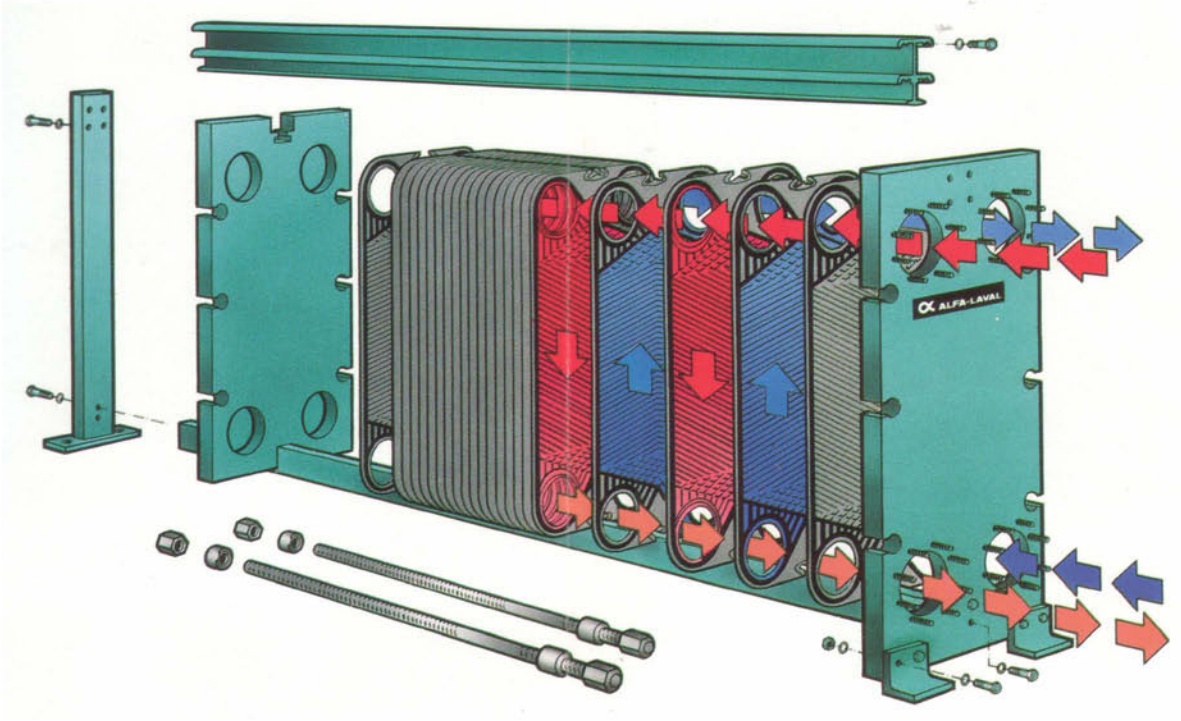

Figure 1.3 Alfa Laval plate heat exchanger, Alfa-Laval (2001)

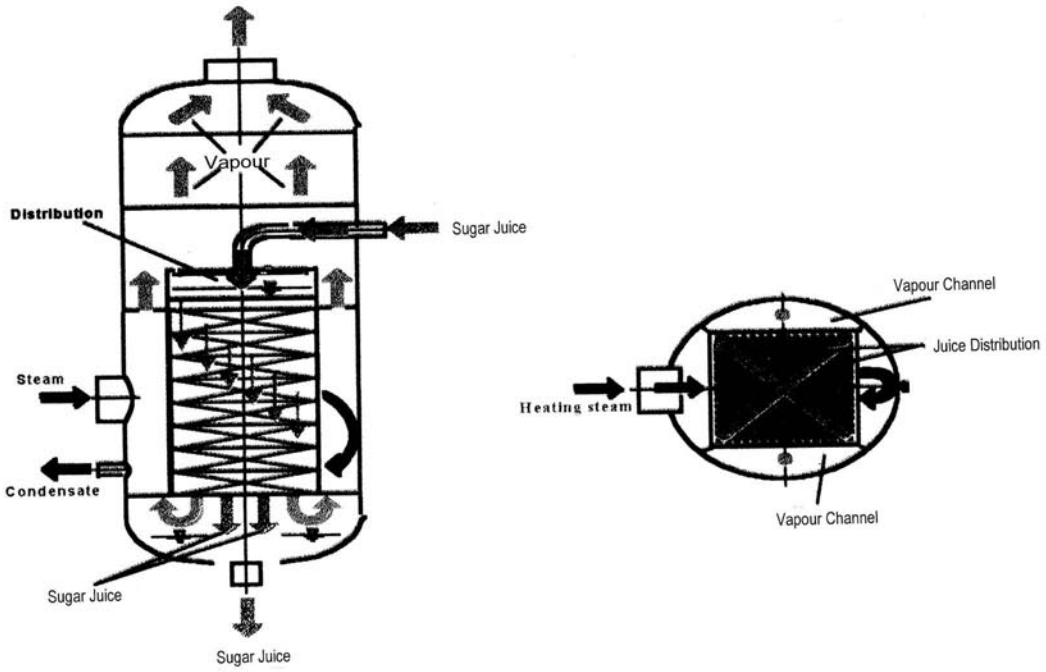

Figure 1.4 Typical plate type falling film evaporator, Grant *et al.* (2000)

1.1.2 Tube type evaporators

Tube type evaporators consist of a series of vertical tubes packed into a heating element called a calandria. Saturated LP steam or vapour condenses on the outside of the tubes while the juice boils on the inside. Tube type, falling film evaporators pump the juice onto a perforated plate above the tops of the tubes and force the juice and the vapour down the tubes. Tube type, rising film evaporators feed juice into the space beneath the calandria, allow the juice to boil inside the tubes and remove the concentrated juice from the bottom of the vessel. Vapour passes up the tubes and into the 'headspace' of the vessel. Similarly the pressure difference between vessels causes the vapour to flow from the headspace of one vessel to the calandria of the next. Figure 1.5, from Watson (1987), shows a typical design of the tube type, rising film evaporator. In the past, several variations of juice entry and exit locations above and below the calandria have been adopted. This gave rise to the terms under and over, when describing the location of the juice inlet and outlet locations, e.g. an under-over configuration would have the juice entry below the calandria and the juice exit above the calandria. By far the most common evaporator in the Australian industry is the tube type, rising film evaporator in the under-under configuration. This type of vessel is referred to in the industry as the 'Roberts' evaporator.

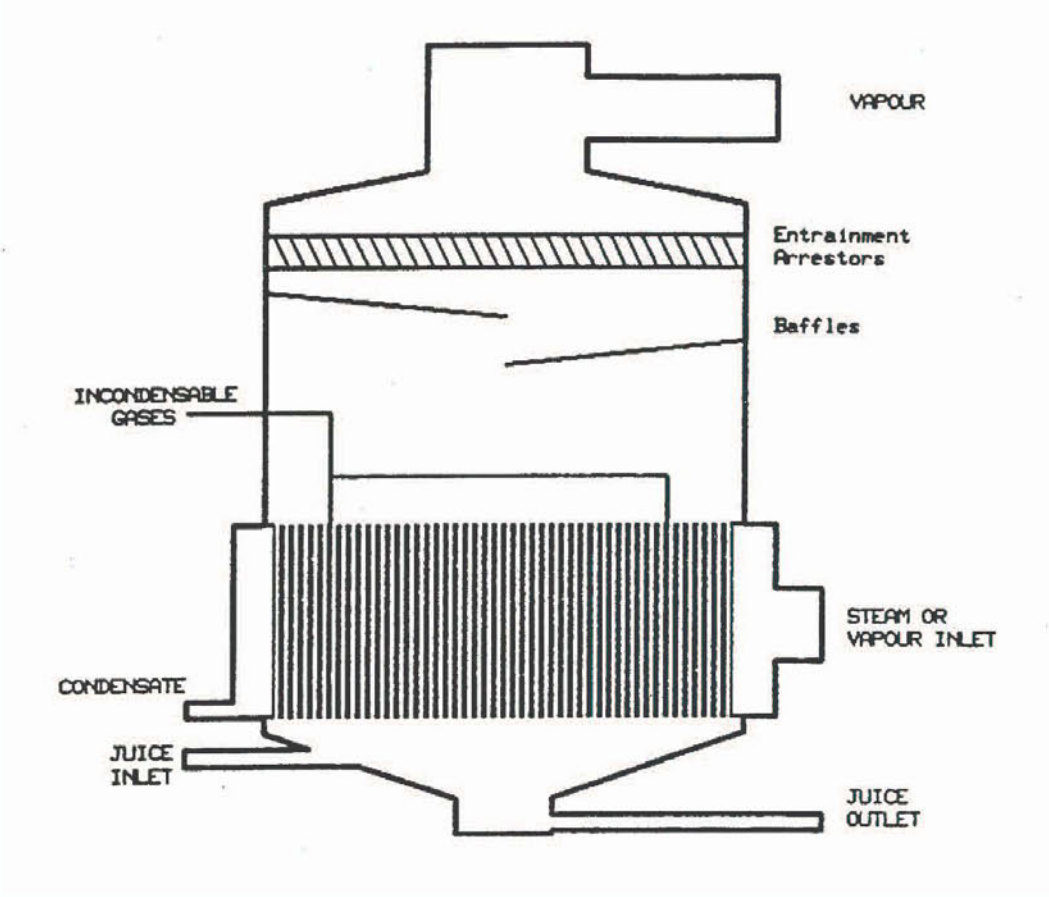

Figure 1.5 Typical Roberts design of evaporator, Watson (1987)

Rural Press Qld (1998) and Rural Press Qld (2001) contain a breakdown of the Australian sugar industry's evaporative capacity in terms of HSA. The Australian sugar industry operates a total of approximately 423 000 m^2 of evaporator HSA. Of this figure over 97% is in the form of the Roberts evaporator, with the remainder being plate type of various descriptions.

Some Australian sugar mills use plate type heat exchangers to preheat the ESJ close to the boiling point before it enters the first evaporator vessel to reduce the amount of sensible heating required in the first effect of the evaporator station. Juice pre-heaters are not included in the scope of this investigation.

The main advantages of the Roberts evaporators are the low cost per unit of HSA, the low maintenance costs, the ease of cleaning including mechanical cleaning if required and the robust control of these units due to the larger buffer volume of juice held in the base of these vessels. DeViana *et al.* (1993) states that the installed cost of a plate type evaporator

is typically in the range of \$450/m^2 to \$750/m^2, depending on the particular installation requirements. Roberts vessels are typically installed for \$350/m^2 to \$450/m^2. In spite of the reduced cost associated with the tube type Roberts evaporators, the material requirements of the tubular type vessels tend to be significantly higher. Figure 1.6a, from Lehnberger (1996), shows the material requirements for the construction of various evaporator types in kilograms of materials per unit of HSA.

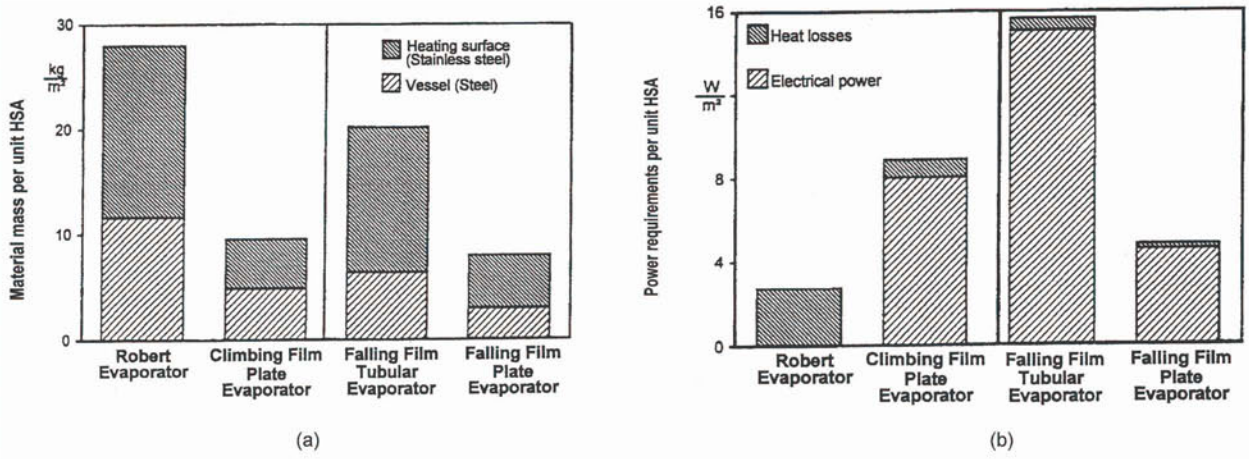

Figure 1.6 Material and power requirements for various evaporator types, Lehnberger (1996)

The other major running cost associated with some evaporators is the electrical power required to drive pumps etc. In most cases the Roberts design requires no pumping capacity, as mentioned previously. Figure 1.6b shows the power costs of various evaporator types.

The HTC of plate type evaporators is generally higher than tubular type evaporators. An increase in the HTC will allow lesser HSA to be installed for the same heat flux (evaporation rate). Thus the capital cost for a given evaporation duty may be reduced for plate evaporators by decreasing the amount of HSA required. This must be taken into account when considering the cost figures quoted previously in AS\$/m^2.

1.2 Evaporator set operation

1.2.1 General principles

Evaporator vessels are configured such that the vapour evaporated in the first effect is used as the heat source for the second effect and so on down the set. Figure 1.7 Wright (1983) shows this configuration pictorially. A temperature difference driving force is required to drive the heat transfer and so the temperature of the vapour at the outlet of the vessel will always be lower than that of the vapour or LP steam used as the heating source. The vapour is recycled in this manner to improve the thermal efficiency of the evaporator set.

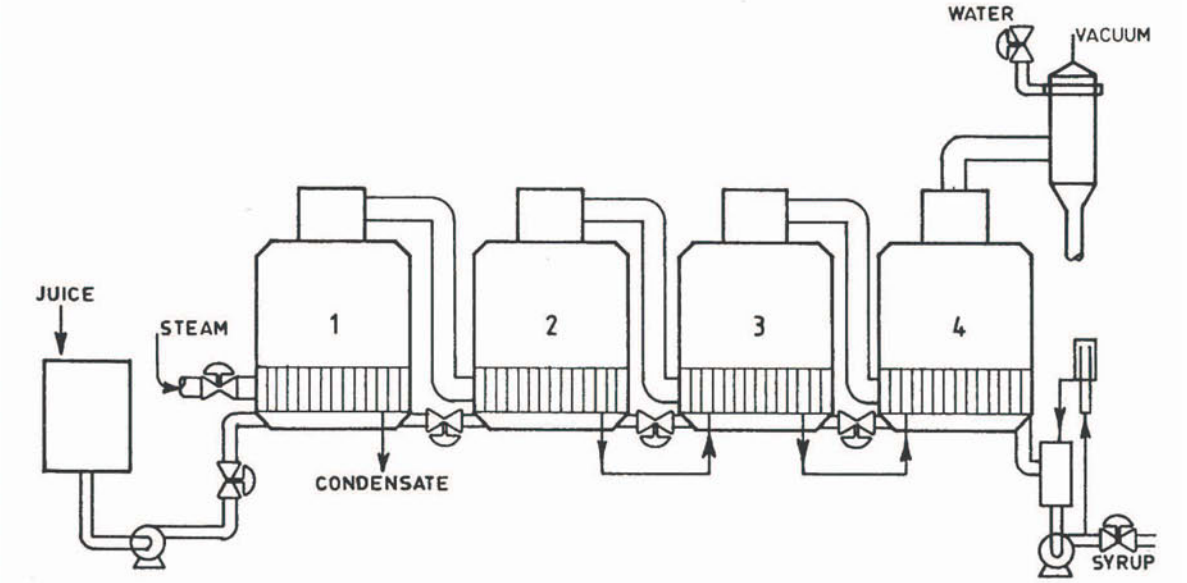

Figure 1.7 Multiple effect evaporation diagram, Wright (1983)

The temperature difference is often used to judge the thermal efficiency of the vessels. LP steam is used as the heat source in the first effect, and is typically at 118 °C to 125 °C in the saturated condition or very slightly superheated, whilst the temperature of the vapour at the outlet of the final effect is usually about 55 to 60 °C at saturated conditions. The pressure in the first effect vessel is determined by the pressure of the LP steam supplied to the evaporator set and in most cases de-superheaters are used to ensure the LP steam is at saturated conditions. The saturation temperature of the vapour at the outlet of the final effect vessel is regulated by controlling the headspace pressure (vacuum) in the final effect vessel(s). Given that the vapour pressure is being controlled by the two extremes, at the

first and last vessel(s) of the set, the pressure of the vapour streams in the remainder of the vessels in the set are left to equilibrate naturally. Many factors influence the equilibrium pressures and these include the heat transfer areas of the vessels in the set, the heat transfer coefficients (HTC), the vapour flow rates, and rates of withdrawal of vapour from individual vessels for other heating duties e.g. juice heating.

Since the 1880s the sugar industry has adopted the principle of multiple effect evaporation because it gives a more efficient usage of LP steam compared with the earlier practice of single vessel evaporation. Wright (1983) states that the LP steam requirement for the evaporation of unit mass of water is approximately (1/n) units, where n is the number of stages. Therefore, LP steam consumption is reduced by the implementation of a larger number of evaporator stages. However, the heating surface area (HSA), and therefore the capital cost, to achieve the required evaporation capacity must increase as more stages are specified. This is due to the reduced temperature difference available across each stage and therefore reduced driving force for heat transfer, then available across each stage. The number of stages chosen is usually that just necessary to achieve the required LP steam economy. The Rural Press Qld (2001) contains data on the entire Australian sugar industry's evaporator HSA. From this data it can be calculated that, at the time of publication, the Australian sugar industry had approximately 86% of its total evaporator HSA in quintuple sets (five evaporation stages), with the remainder in quadruple sets (four evaporation stages).

LP steam is used for heating duties in the juice pre-heaters and pans in different parts of the factory. Some of the vapour produced by the evaporators can be bled off and used to substitute LP steam for these heating duties. This process is called vapour bleeding. By doing so the overall LP steam consumption of the factory is reduced resulting in increased export of electricity to the grid. Decreasing the temperature difference and therefore increasing the temperature of the vapour produced, increases the suitability of the bleed vapour for alternate uses.

In an evaporator set that has a balanced distribution of HSA across all of the effects and has no vapour bleeding, the quantity of water removed from the juice by evaporation in each effect is approximately the same. Since the amount of solids flowing through the set does not change, the relative quantity of vapour removed per unit volume of juice increases further down the set. Therefore, the brix increase from inlet to outlet in the later effects is always greater than in the earlier effects. Figure 1.8, from Attard (1991), shows this brix increase diagrammatically. Vapour bleeding shifts the evaporation loading and the

magnitude of the increase in brix of the juice from the vessels located after the bleed point to the vessels located before the bleed point. See Appendix A for further clarification of the term brix.

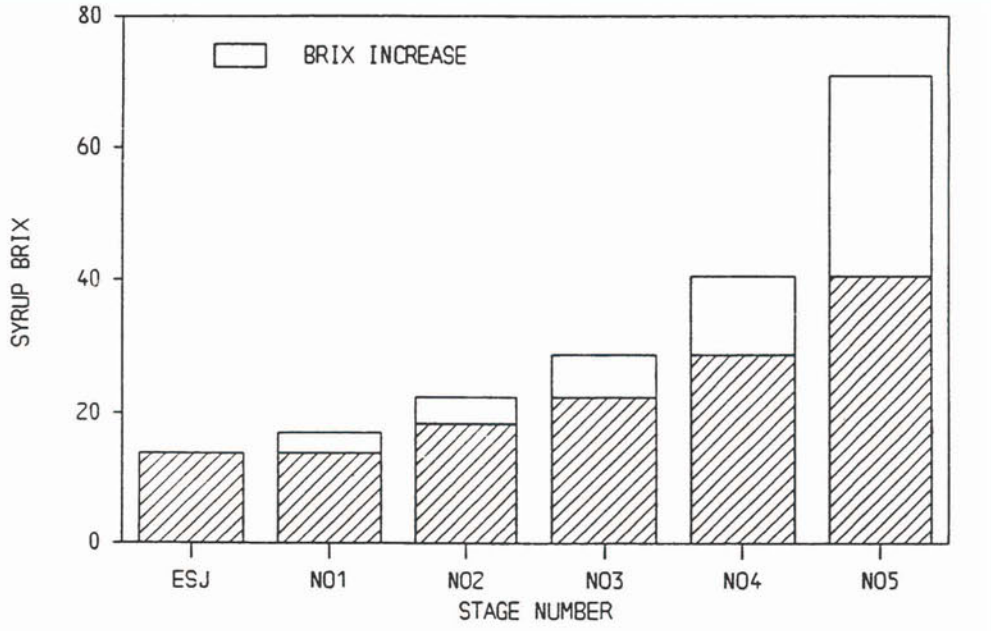

Figure 1.8 A typical evaporator brix profile, Attard (1991)

1.2.2 Co-generation

Opportunities for factory co-generation are increasingly seen as necessary for maintaining the economic viability of the cane sugar factory. Decreasing the amount of LP steam required for processing increases the likelihood of alternative uses for the steam, such as the production of electricity. Evaporation and juice heating systems dominate energy use in the raw sugar factory. Wright (2000) investigated possible options for the reduction in LP steam consumption in the raw sugar factory. This investigation found that vapour recompression is not suitable for increased co-generation but vapour bleeding and good housekeeping (e.g. fixing leaks, etc.) are suitable. Direct contact juice heating has the advantage of being able to reduce the approach temperature (the temperature of the heating vapour less the temperature of the juice being heated) but has the disadvantage of requiring a larger evaporative capacity due to increased water consumption.

In the past the LP steam consumption of raw sugar factories has been determined by balancing the bagasse consumption with bagasse production, so as to minimise bagasse

disposal costs. According to Wright (2000), Australian factories typically operate with steam mass flow rates within the range of 46% to 60% of the cane mass flow rate as it enters the factory. This value is termed the steam on cane. However, overseas experience has demonstrated that steam consumption can be reduced to below 30% steam on cane by employing LP steam economy measures. 30 % steam on cane is considered the current practical minimum steam consumption that can be achieved economically. Lower steam on cane can be achieved but the cost of installation and operation currently exceeds the cost of supplementing the fuel supply with fossil fuels.

Some of the more commonly used options for reducing steam consumption in the factory along with advantages and disadvantages for each, are listed as follows:

1. ***Use of electric or hydraulic drives on the milling train.***

Advantages:

- All of the HP and LP steam pipes are removed from the milling train, thus reducing the potential for leaks,
- HP steam available for co-generation is maximised, and
- The factory requires only one turbine to drive the generator thus reducing the capital cost associated with turbines.

Disadvantages:

- Hydraulic and electric drives are very expensive to install initially,
- Removing the existing turbines on the milling train does not effectively utilise the existing plant and thus increases the capital cost associated with installation,
- Hydraulic and electric drives have significantly higher maintenance costs than existing steam turbines, and
- Previous installations of hydraulic drive technology in Australian factories have encountered problems such as wear on internal components.

2. ***Membrane technology for concentrating the juice rather than heating.***

Advantages:

- The most significant consumer of LP steam in an existing factory, the evaporator station, is completely removed and replaced with technology that consumes no LP steam at all, and
- The amount of HP steam available for power generation is significantly increased.

Disadvantages:

- Membrane technology is extremely expensive to purchase, install and operate,
- The pumping requirements of the membrane plant are a significant consumer of electrical power. Even though the total amount of power generated is increased the net amount exported to the grid is not necessarily a significant amount, and
- Membrane technology is unproven, on a large scale, in the sugar industry and thus uptake is slow.

3. ***Vapour bleeding from the evaporator station for heating duties elsewhere in the factory.***

Advantages:

- The overall efficiency of the process is being improved by replacing LP steam with what would normally be regarded as a waste product,
- The cost of retrofit is reasonably low,
- The existing plant is still being utilised thus decreasing the capital cost of installation, and
- The technology is well proven in both the Australian sugar industry and in other overseas sugar industries.

Disadvantages:

- The requirement for LP steam to perform heating duties is only reduced it is not completely removed, and

- Vapour bleeding creates large instabilities in the operation of the evaporator set and complicated control strategies are required to overcome this.

For the reasons stated above, the most common option employed in Australian factories is the use of vapour bleeding from the evaporator station. The use of vapour bleed systems has consequences for the evaporator station in that it is desirable to produce hotter vapours. Figure 1.9, from Wright (2000), shows a generalised evaporator/heater/vacuum pan vapour system for improved LP steam economy. Figure 1.9 shows the use of vapour from the first effect (vapour one) being used for clarified and secondary juice heating and for use on the pan stage. Vapour from the second effect (vapour two) is used for secondary juice heating and for use on the pan stage. Vapour from the third effect (vapour three) and vapour four is used for primary juice heating whilst the vapour from the fifth and final effect is passed into the condenser. The limitations on the system are that the final effect vapour pressure must be maximised and the LP steam supply to the first effect must be minimised, in order to obtain the optimum LP steam consumption. In this case the vessels are required to operate with higher HTC and lower effective temperature difference than would normally be experienced in factory operations. These performance indicators are discussed later in section 1.3.3.

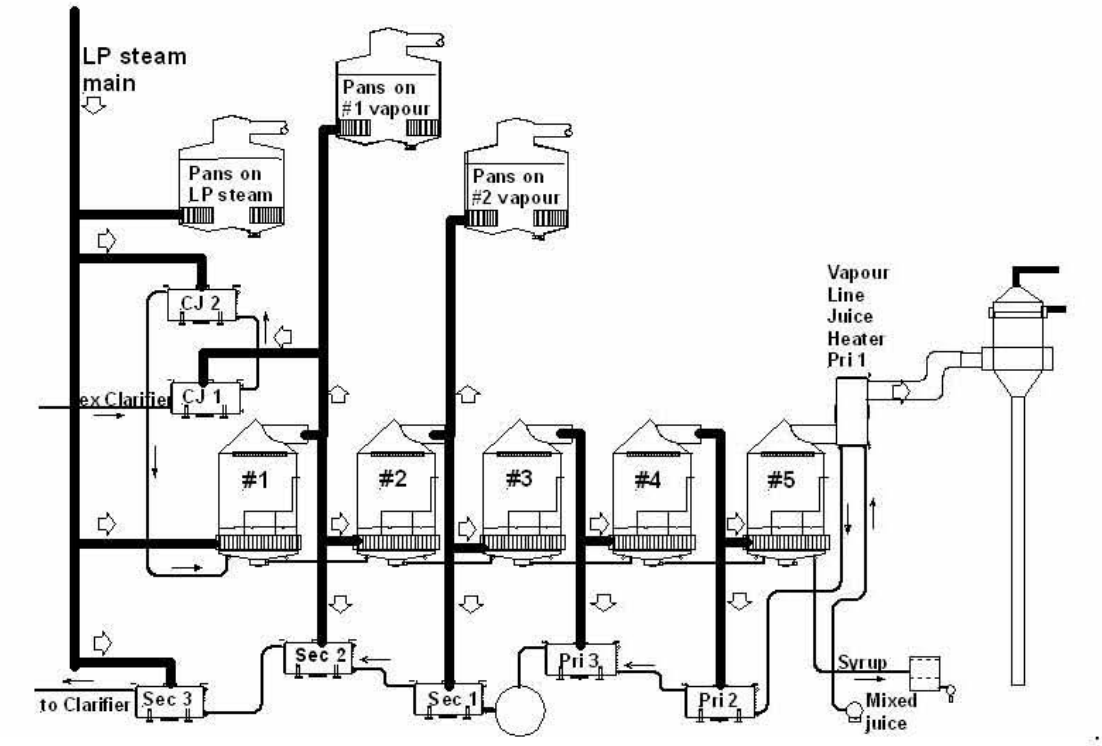

Figure 1.9 Generalised evaporator/heater/vacuum pan vapour system for improved LP steam economy, Wright (2000)

1.3 The Roberts vessel

1.3.1 The basic design

Wright (1983) states that in Australian practice the evaporator vessels are of mild steel construction and use 18 gauge stainless steel (grade 304) tubes, from 1.6 m to 2.5 m in length, and 38 mm to 54 mm outside diameter. This is supported by the data seen in Bureau of Sugar Experiment Stations (BSES) (1992). The data published in this reference is a comprehensive listing of the evaporating plant found in all Australian raw sugar factories. An analysis of this data reveals that the most common tube size is 44.45 mm outside diameter (OD), with 63% of the total number of vessels in the industry having tubes of this diameter. Of the vessels with 44.45 mm OD tubes, almost 84% were made from stainless steel. Of all the vessels with 44.45 mm OD, stainless steel tubes, 48% of vessels contained tubes with a wall thickness of approximately 1.2 mm and had an average tube length of approximately 1.98 m. The shortest tube length was 1.53 m and the longest tube length was 2.70 m.

This source of data is still considered to be the most reliable at present. The equipment found in factories is not expected to have changed substantially during the time since 1991.

1.3.2 Vapour side operation

While there have been, and still are, many variants of the Roberts vessel, the operating principles have remained virtually unchanged. LP steam or vapour from the previous effect is fed into the calandria, through one or two inlet pipes, and condenses on the outside of the tubes. The condensate is removed from the bottom of the calandria and is usually pumped to a common condensate tank. The location of the condensate outlet varies depending upon the design and in some cases there may be more than one outlet point. Small amounts of air and other non-condensable gases are always present in the flow on the vapour side of the calandria. These gases are removed through vent pipes located within the array of calandria tubes. The location of the non-condensable gas vents varies significantly between designs.

Gaps between the calandria tubes, called steam lanes, and baffle plates are often incorporated into the calandria design. These steam lanes and baffles assist in the dispersion of vapour around the calandria. The purpose of the steam lanes is to provide a path of lesser resistance for the vapour flow to those areas that may otherwise receive little flow. Baffles are used to divert the vapour flow to different areas around the calandria and towards the non-condensable gas take off points. Figure 1.10a, from Peacock (1999),

shows a branch type steam lane configuration installed in one of the Roberts vessels at the Proserpine Mill. In this design the vapour flow is predominantly down the lane in the middle of the vessel and branches out towards the exterior of the vessel. This type of vapour distribution system has no obvious point at which the non-condensable gasses will accumulate. Consequently the gas is removed from points throughout the calandria.

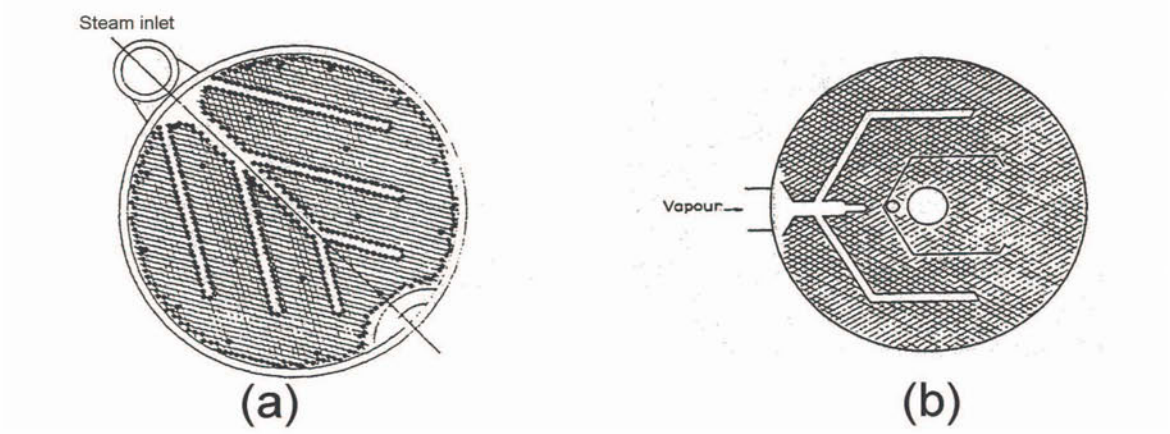

Figure 1.10 Steam lane and baffle design in Roberts evaporator vessels, Peacock (1999)

Baffles have also been used to provide a more defined path for the vapour flow through the calandria. Figure 1.11, from Peacock (1999), shows two baffle designs. The zigzag baffle configuration has a higher pressure drop due to the sudden changes in direction but the helical baffle configuration has a longer path to travel.

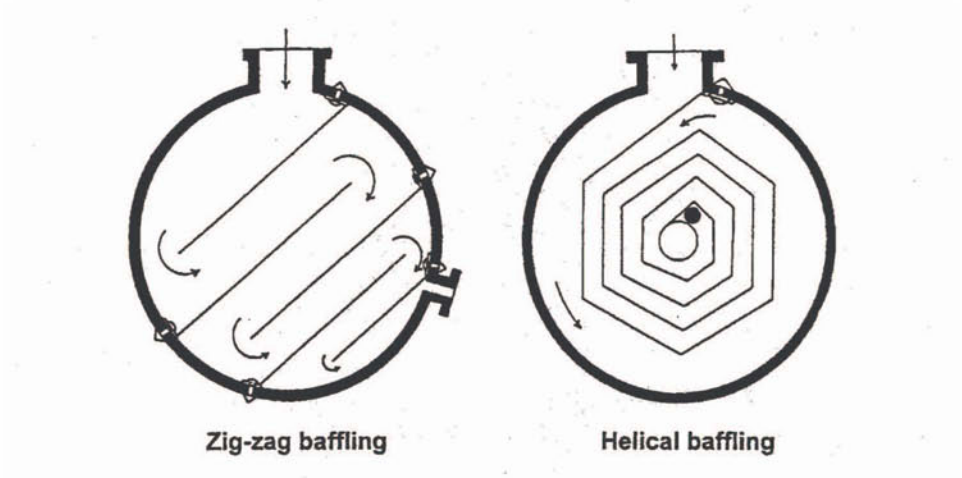

Figure 1.11 Types of baffles in Roberts evaporator vessels, Peacock (1999)

Baffles and steam lanes can both be used on the same vessel in order to combine the improvements of both concepts. Figure 1.10b shows one calandria design incorporating steam lanes and baffles. Although the vapour flow path shown in Figure 1.10b is not as well defined as that in Figure 1.11, the non-condensable gasses are tapped off from a single point.

Another method of obtaining a more uniform vapour distribution within the calandria is to vary the tube layout. Tubes spacings predominantly have a rhombic (symmetrical) layout comprising of two equilateral triangles having 60° angles between sides. Tromp (1966) discusses a large variety of different tube layout designs and the effect on vapour flow around the outside of the tubes. Figure 1.12, from Tromp (1966), shows varying pitch tube spacing. In this configuration the portion of the tube bank closest to the vapour entry, approximately two thirds of the total tube-plate area, has a pitch that is 15% larger than the remainder. This encourages the vapour to evenly distribute throughout the calandria by providing a large area of lower resistance to the flow. The vapour then passes over the remainder of the tubes that have a smaller pitch. Figure 1.12 also shows a vessel with a central downtake on the juice side. Downtakes will be discussed in further detail later.

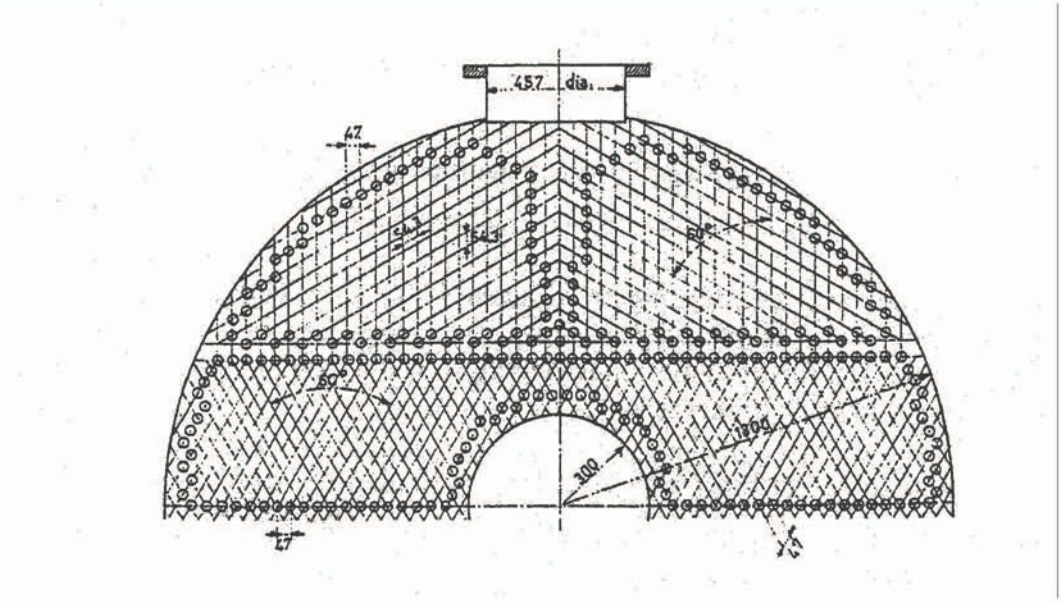

Figure 1.12 Variable tube pitch calandria, Tromp (1966)

The vapour inlet system can also take the form of a belt around the outside of the vessel with a large number of smaller inlets into the calandria. Figure 1.13, from Peacock (1999), shows the vapour flow path around the belt. In this configuration the vapour does not enter

the calandria directly from the inlet pipe. Instead it is first passed through an annular space, or belt, around the outside of the vessel. The belt has the purpose of evenly distributing the vapour around all of the inlets into the calandria. The vapour flow is predominantly radial in this case and has the advantage of a defined flow path, and therefore a defined tapping point, for the non-condensable gases. Non-condensable gases and condensate are removed from the centre of the vessel. This configuration can be used without the aid of steam lanes for flow distribution, but often steam lanes are included to ensure even vapour distribution.

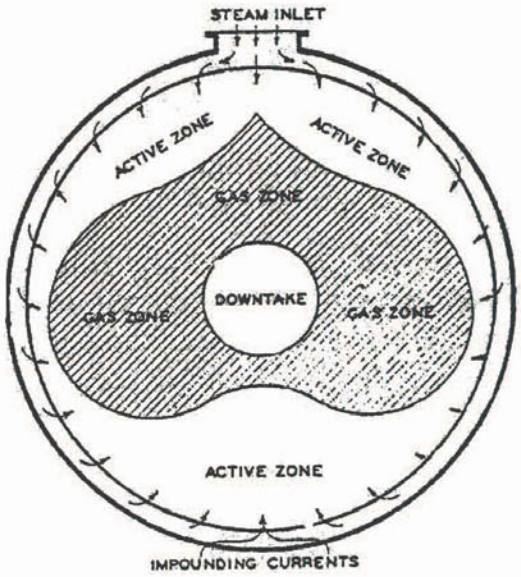

Figure 1.13 A circumferential belt producing radial vapour flow, Peacock (1999)

1.3.3 Juice side operation

The basis of operation for the Roberts vessel is to feed juice into the space under the calandria of the vessel, usually from three or four points, and to withdraw juice through an outlet usually located close to the centre of the vessel. Some vessels employ baffles and other such devices to avoid short-circuiting but most will not. The juice is drawn up through the heating tubes once boiling is initiated. The vapour fraction increases towards the top of the tube and forms a small layer of 'froth' above the top tube-plate. This mixture of juice and vapour above the top tube-plate is usually in the order of 150mm high. The static juice level within an evaporator is typically within the range of 30% to 60% of the tube height.

The vapour released from the boiling liquid travels up from the calandria and into the headspace of the vessel. At the top of the vessel are entrainment arrestors, usually of the louvre type, to prevent the carry-over of liquid droplets into the calandria of the next evaporation stage. Since the detailed operation of the entrainment arrestors is outside the scope of this investigation, Wright (1988) and Henderson *et al.* (1981) should be referred to for further discussion on the topic.

Evaporator operators will typically use the height of fluid above the top tube-plate as a means of controlling the operation of the vessel. Watson (1987) suggests that theoretically, the height of fluid above the top tube-plate should be minimised so as to reduce the static head above the boiling tube. However, the top tube-plate should not be allowed to dry out, as caramelisation of the sugar solution will occur. This concept is supported by experiments carried out by Guo *et al.* (1983) on a three-tube evaporator test rig. The test rig included an external leg to allow juice to return from above the top tube-plate to the space below the calandria. The downtake also included a valve so that the flow could be restricted and the static fluid height above the top tube-plate could be varied. It was found that the greatest HTC was achieved when the boiling juice was just wetting the top surface of the tube-plate. The test rig was operating under ideal conditions and the test results would suggest that the evaporator operators are incorrect in maintaining a static fluid height of approximately 150mm above the top tube-plate. However, less than perfect conditions and instabilities within the factory would account for the need to increase the height of the fluid above the top tube-plate when operating a full-scale vessel under factory processing conditions.

Watson (1987) states that industry vessels generally do not have any means of returning the juice to below the calandria and it is assumed that those tubes which are boiling less intensely than average, act as downcomers. Watson (1987) also states that this effect could indeed be cyclic and cause instabilities in the fluid layer above the top tube-plate. Tubes could be boiling rapidly at one point in time and fluid could be flowing up the tube, while a short time later (perhaps a few seconds only), the boiling could have subsided and the tube could be acting as a downtake. No reference material has been located at this point in time to support or disprove this hypothesis. However, observations of the boiling surface in factory evaporators indicate that cyclic boiling behaviour, with regions changing from intense boiling to induced flow, is common. This may explain why factory vessels are operated at a static fluid level that is slightly greater than that found by Guo *et al.* (1983) in their test rig experiments.

Quinan *et al.* (1985) discussed the design of a 5100m^2 evaporator installed at the Fairymead Mill during the 1984 crushing season. The calandria layout for this vessel contained many steam lanes and the multiple downtake locations within the tube layout. Watson (1987) investigated the effect of downtakes for reducing the fluid head above the tubes.

Watson (1986a) further discussed the performance of the Fairymead evaporator from Quinan *et al.* (1985). A practical and well thought out approach by Watson (1986a) stated that a large number of smaller downtakes were thought to reduce the liquid level more effectively than a single central downtake, due to the very large diameter of the vessel. Watson (1986a) also highlighted that multiple downtakes have the added advantage of replacing the mechanical stays used to hold the top and bottom tube-plates.

Watson (1986a) quantified the effect of the downtakes on reducing the head in the Fairymead evaporator, by measuring the head of fluid above the top tube-plate with a differential pressure level transmitter. The testing of operating scenarios, with and without downtakes was achieved by blocking the downtakes with plumbers' expandable plugs, installed during a scheduled maintenance stop. The results of the tests took the form of a plot of head above the calandria versus level of juice in the tubes. Figure 1.14 from Watson (1986a) shows that there is a noticeable difference in the head with downtakes. The next logical step is to relate the effect of the downtakes to heat transfer performance by plotting the HTC for the two cases. Figure 1.15, from Watson (1986a), shows that the HTC with downtakes was approximately 250 $W \cdot m^{-2} \cdot K^{-1}$ higher than the corresponding HTC without downtakes, at the peak value. It should be noted that there is a lot of scatter in the data and Watson (1986a) makes no mention of accuracy in his discussion.

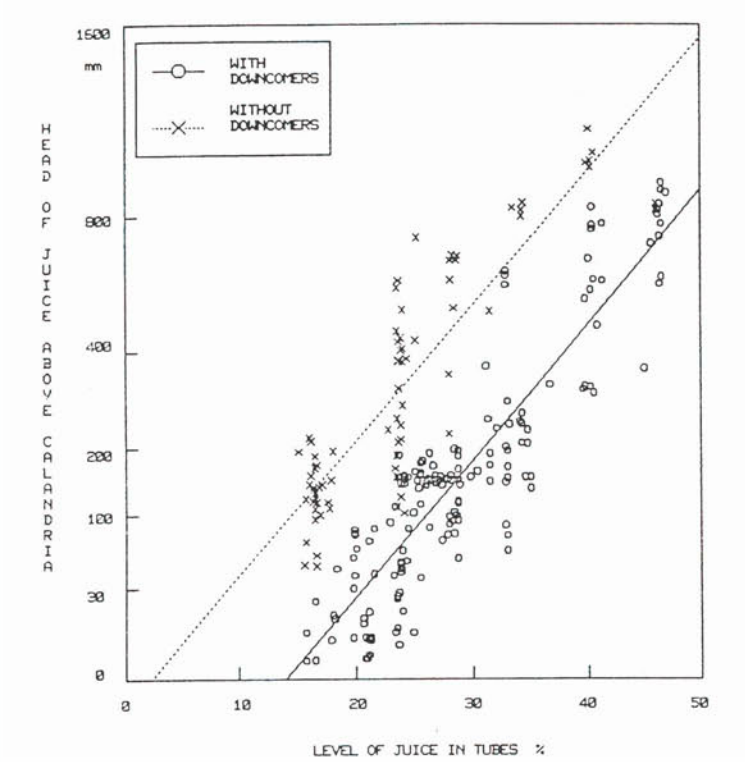

Figure 1.14 Plot of juice head above the calandria versus level of juice in the tubes, Watson (1986a)

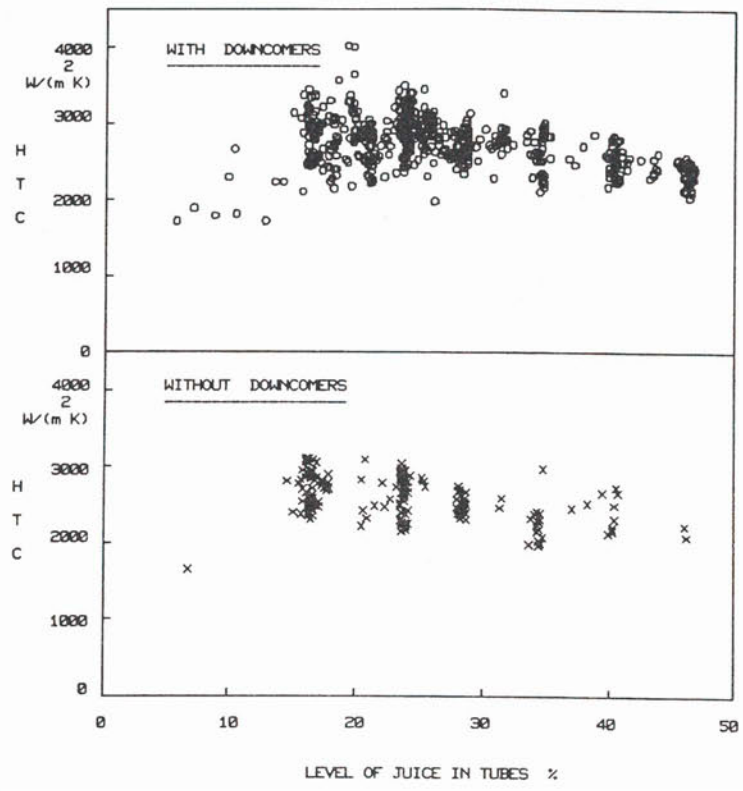

Figure 1.15 Plot of HTC with and without downtakes, Watson (1986a)

Those parts of the vessel that come into contact with the boiling juice tend to form a scale, particularly on the inside of the heating tubes. This scale acts as an insulator and therefore decreases the heat transfer performance of the evaporators over time. Various processes, usually involving the boiling of caustic soda or other such chemicals, remove scale periodically. Significant amounts of work in the area of scale removal and prevention have been done and there is a large amount of literature present. Doherty (2000) and Ivin and McGrath (1990) discuss the removal of evaporator scale using chemical cleaning processes. Crees (1983) and Abernethy *et al.* (1991) discuss the use of scale inhibitors. These references should be sought for further detail on evaporator scale. The insulating properties of scale must be taken into account conducting factory experiments. The scale formation process and its removal are outside the scope of this investigation.

1.4 Evaporator performance

An overall HTC (U) is used to quantify the heat transfer performance of evaporators. It is found by measuring the overall heat flow through the calandria (Q) and averaging it over the entire HSA of the vessel (A) multiplied by the effective temperature difference between the hot and cold fluids (ΔT), as per equation (1.1).

$$U = \frac{Q}{A\Delta T} \qquad \textbf{(1.1)}$$

Table 1.1, from Watson (1986), shows typical HTC values for each effect in an evaporator set. This method does not make any allowance for localised areas of high or low heat transfer, nor does it allow for the changes in heat transfer over the length of the tube.

Table 1.1 Typical values of HTC for different effects, Watson (1986)

Effect No.	Typical HTC ($W \cdot m^{-2} \cdot K^{-1}$)
1	2960
2	2470
3	2090
4	1550
5	610

The head of juice within the tube and the different boiling regimes experienced within the tube are expected to cause significant variation in HTC along the length of the tube. This method also assumes even LP steam or vapour distribution throughout the calandria. In

practice poor design of steam lanes and non-condensable gas removal systems (as discussed previously) will cause uneven heat transfer in different sections of the calandria. Whilst this method is considered adequate for performance evaluation for factory type operation, it is considered inadequate for an in depth study such as the development of a CFD model and understanding of the flow regimes within the tube.

The total heat flow through the calandria (Q) used in equation (1.1) must take into account any sensible heating of juice prior to the commencement of boiling and also any flashing of vapour from the juice at the inlet of the vessel. Appendix A to Broadfoot and Dunn (2001) details how these effects are accounted for in the calculations.

The effective temperature difference (ΔT) used in equation (1.1) is the difference between the saturation temperature of the LP steam or vapour in the calandria and the average temperature of the boiling juice. The saturation temperature of the calandria side is used regardless of the presence of superheat, as in the first effect. As water is evaporated from the boiling juice, the boiling point temperature is elevated above that for pure water at the same pressure. The boiling point elevation temperature (BPET) is described as the actual temperature of the boiling juice less the saturation temperature of water vapour at the headspace pressure. Batterham *et al.* (1973) published equations (1.2) to (1.5) below.

First evaluating BPET at atmospheric pressure ($T_e^{'}$), where $\frac{S}{W}$ and $\frac{I}{W}$ are the sucrose to water and impurities to water ratios respectively:

$$T_e^{'} = 2.442\frac{S}{W} - 0.757 + 3.333\frac{I}{W} \qquad \textbf{(1.2)}$$

Where DS is the dry substance and P is the purity, it can be noted that:

$$\frac{S}{W} = \frac{DS}{(100 - DS)} * \frac{P}{100} \qquad \textbf{(1.3)}$$

$$\frac{I}{W} = \frac{DS}{(100 - DS)} * \frac{(100 - P)}{100} \qquad \textbf{(1.4)}$$

Then evaluating BPET at the pressure under consideration (T_e):

$$T_e = \frac{T_s^2}{\left(\frac{373^2}{T_e'} + (373 - T_s)\right)} \qquad (1.5)$$

Although there are numerous equations for calculating BPET, the most commonly used is that of Watson (1986). These equations are a simplified version of Batterham *et al.* (1973) such that equation (1.5) remains the same and equation (1.2) becomes:

$$T_e' = -0.1379 + 2.22\left(\frac{B}{(100 - B)}\right) + 0.118\left(\frac{B}{100 - B}\right)^2 \qquad (1.6)$$

Watson (1986) does not state the accuracy or the valid range of (1.2), (1.5) or (1.6). Watson (1986) also quotes personal communications with Batterham in his reference list and thus makes it very difficult to cross check the published equations. The most noticeable difference between the equations is that those published by Watson (1986) do not include the purity terms as per Batterham *et al.* (1973). No explanation for this difference can be offered at this stage. One suggestion is that the equations published by Batterham *et al.* (1973) are generic and were designed for use in pans where the purity of massecuite and molasses changes significantly. Since the equations published by Watson (1986) are designed for use in evaporators, where the purity does not change significantly, it is possible that a typical value for purity has been assumed and substituted into the equations in order to simplify them.

The term brix (B), as used in equation (1.6), is different to the dry substance (DS), see Appendix A for definitions, but the two values are sometimes interchanged since both are a measure of the amount of solids in a solution. The dry substance is a measure of both soluble and insoluble solids present in the solution by weighing and drying in an oven. Dry substance is neither temperature nor purity dependent. The brix can be measured using a hydrometer (spindle brix) or by refractive index (refractometer brix). The spindle brix method measures the specific gravity of the solution. The variation of the properties of the solution from that of water is then related to the amount of solids present in the solution. Refractometer brix measures the refractive index of the solution and again the variation in the properties is related to the amount of solids in the solution.

Brix measurement is dependant on the temperature of the solution and is therefore quoted at a reference temperature. eg. a 20 brix solution at 20 °C. Since the degrees brix expressed is the mass % of sucrose in a pure aqueous sucrose solution, there is no real temperature effect. The difference appears in the measurement since the instruments are calibrated at a given temperature ie. 20 °C. The Lab Manual by The South African Sugar Technologists' Association (1985) provides further clarification of the difference between the two methods.

Since the analysis of a sample for dry substance requires laboratory equipment and large amounts of time, this value is sometimes not used for studies involving large numbers of samples. Brix measurement is faster and easier and the difference between brix and dry substance is small. However, dry substance provides better data and this must be considered when designing a test procedure.

Due to the elevation of the boiling point temperature of the juice the water that is evaporated from the juice is at the headspace pressure but at the juice temperature. Therefore, the vapour released from the boiling juice contains an amount of superheat equal to the BPET. Although it must be noted that this is often neglected due to the insignificant amount of heat energy contained in the superheat as compared to the latent heat.

The evaluation of heat transfer performance in evaporators must take into account the effect of juice sub-cooling and / or juice flashing at the inlet. If these effects are not taken into account the HTC calculated will contain significant error. This can be done by a simple enthalpy balance on the juice flow at the inlet to the vessel under evaluation.

When a vessel has superheat in the calandria the heat flow due to sensible cooling back to saturated conditions is generally taken into account if there is more than 20 to 30 K of superheat. However, the effective temperature difference is still calculated using the saturation temperature of the incoming vapour or LP steam. This assumption is considered sound since the superheated vapour coming into contact with condensation on the outside of tubes will vaporise the condensate back and in doing so will cool itself closer to the saturation temperature and will eventually begin condensing. Therefore, it is the release of the latent heat from the vapour or LP steam condensing on the outside of the tube that provides the majority of the heat source to the tubes.

1.5 Numerical modelling

There have been very few attempts at numerical modelling of sugar mill evaporators. A small number of attempts have been made at modelling of vacuum pans and some comparisons can be made between the two but the differences must be considered carefully.

1.5.1 Steindl and Ingram

Steindl and Ingram (1999) completed a comprehensive study of many facets of the Roberts evaporator. The study included factory experiments to determine the HTC and residence time distribution (RTD) of the Proserpine evaporator station. The study also included details of how the CFD package FLUENT, was used to model the flow in the Proserpine #1b vessel.

The CFD part was very limited in its application in that it only examined the juice flow in the region below the calandria. Although the project sought to investigate multi-phase flow in tubes, the boiling of juice in a single tube was not considered. Instead it was simply stated, "Various strategies to represent boiling and condensation in FIDAP were tried but they were met with little success". With regard to FLUENT 4.4.7 "Stephens and Harris (1998) later reported that FLUENT's gas-liquid multiphase flow and phase change calculations are incorrect, and cannot be used to model boiling. Further work on the detailed modelling of boiling and condensation processes was not undertaken". Steindl and Ingram (1999) did not mention any details of the methods employed, include any discussion or make any comment about the direction future modelling work on boiling inside a tube should take.

When modelling the juice flow beneath the calandria, Steindl and Ingram (1999) made a number of simplifying assumptions. The evaporator was modelled as a 60^{o} segment of the juice space below the calandria with the top of the wedge being the bottom tube-plate. Boundary conditions were then applied to the top surface in order to represent the action of the heating tubes without explicitly modelling them. The top surface was frictionless and was a mass sink for the water component of the sugar solution. The mass flow rate of water through the boundary was calculated based on the average evaporation rate of the vessel.

Neglecting the boiling action inside the heating tubes and the effect it would have on the remainder of the fluid flow is considered to be the most significant shortcoming in the work of Steindl and Ingram (1999). The boiling action inside the heating tube will do more than to simply remove water from the sugar solution at the bottom of the tube. It is likely that

the boiling action will affect the velocity and pressure distribution within the fluid directly underneath the bottom tube-plate. This area is seen as the largest potential for improving the accuracy in model predictions. To date, no attempts to model or to understand the boiling action inside evaporator heating tubes have been located.

The sugar solution was modelled as a two-component fluid consisting of water and dissolved solids. As the water component was allowed to leave through the top surface the concentration of the sugar solution remaining increased. This allowed the model to predict the brix increase as the fluid flowed through the vessel. The model also included the effects of gravity and buoyancy effects resulting from the change in fluid density experienced as the concentration of the fluid increases.

Taking advantage of vessel symmetry is often required in order to reduce the computational run times required to arrive at a converged solution. Steindl and Ingram (1999) reported excessive run times but did not quantify the size of the model or provide details of the computer used. A 60^{o} wedge was used to reduce the size of the model that would have significantly reduced the computer resources required.

Steindl and Ingram (1999) used the following boundary conditions on their model:

- **Juice entry:** velocity inlet type boundary condition, inlet velocity components and turbulence parameters, inlet juice brix;
- **Juice outlet:** zero pressure drop type boundary condition;
- **Vessel walls, floor and internal deflector disk**: no slip wall type boundary condition;
- **Vertical planes bounded by 60^{o} segment**: symmetry type boundary condition; and
- **Top horizontal surface, bottom of the calandria**: volumetric mass sink.

A finite volume approach was used to solve the necessary equations and the standard $k-\varepsilon$ turbulence model was used. Given that the effects of buoyancy were being modelled, corrections to the momentum equation for the term associated with the vertical direction must have been included. However, Steindl and Ingram (1999) do not clearly state how these equations were manipulated or solved. It is suspected that the default settings of the code were used without a detailed understanding.

Comparing the brix at the outlet of the vessel only validated the model. The evaporation rate, was altered until the outlet brix was correct. Although the juice temperature at the vessel inlet was an input to the model, no mention was made of the juice temperature at the outlet. This is considered an important parameter for model validation. Although brix profiles and velocity profiles were used as model predictions, no mention of any validation for internal velocity and brix profiles was made. Experience with $k-\varepsilon$ models has shown that validation of fluid velocities at points other than at inlet and outlet must be done. This is due to the problems that this type of model has in predicting slow moving flows when the inlet and / or outlet velocities are high. Although Steindl and Ingram (1999) did identify the limitations of the $k-\varepsilon$ models with slow moving regions, no mention was made of any verification or corrections to the model predictions.

Problems with standard $k-\varepsilon$ models arise when some parts of the fluid flow are genuinely turbulent and others are laminar or transitional. The models apply turbulence intensity everywhere in the fluid flow and thus cause those areas in the flow that would otherwise be laminar to be treated as turbulent. This causes the fluid flow predictions in these regions to be incorrect. This problem can be accounted for by using more complicated models, such as the Launder-Saito correction, that make allowances for these problems.

The outcomes from the modelling work of Steindl and Ingram (1999) show that a plug flow regime is favourable for evaporator performance. To achieve plug flow a system of peripheral feed, central outlet was recommended. Steindl and Ingram (1999) provided details of two possible designs specifically for the vessels considered in the study. Figure 1.16, from Steindl and Ingram (1999), shows the predicted velocity profile for an evaporator vessel with peripheral feed and central outlet. Figure 1.16 shows a small recirculation zone immediately above the floor of the vessel. This recirculation is undesirable since it reduces the volume of fluid flow available to the heating source for evaporation. Modifying the inlet configuration and the slope of the vessel floor may help reduce the strength of this recirculation. CFD modelling of different geometries will provide details of possible configurations.

Figure 1.17, from Steindl and Ingram (1999), shows the predicted brix profile for an evaporator vessel with peripheral feed and central outlet. This brix profile is desirable because it avoids short-circuiting of low brix juice from the inlet to the outlet. Also the lowest brix material, and therefore the highest local evaporation rate, is on the outside periphery of the calandria. This will provide a larger overall evaporation capacity of the vessel since the HSA of the vessel increases as the radial position away from the vessel

centre increases. Figure 1.18, from Steindl and Ingram (1999), shows the predicted local evaporation rate plotted against the radial position within the vessel. Figure 1.18 shows a significantly larger local evaporation rate at the periphery of the vessel when compared to the centre of the vessel.

The concept of peripheral feed, central outlet is the most significant outcome from the study and this can be achieved in many ways. CFD modelling is seen as a powerful tool for the fine-tuning of inlet and outlet configurations, the design recommended is considered to be an excellent starting point for further modelling.

Even though the work to date has been limited in its scope and has contained significant simplifying assumptions, advances in evaporator design have already come to light using the CFD techniques. CFD techniques have been successfully used for the modelling of sugar mill clarifier vessels and boilers. The application of similar techniques to sugar mill evaporators will provide valuable tools when improving the design of such vessels.

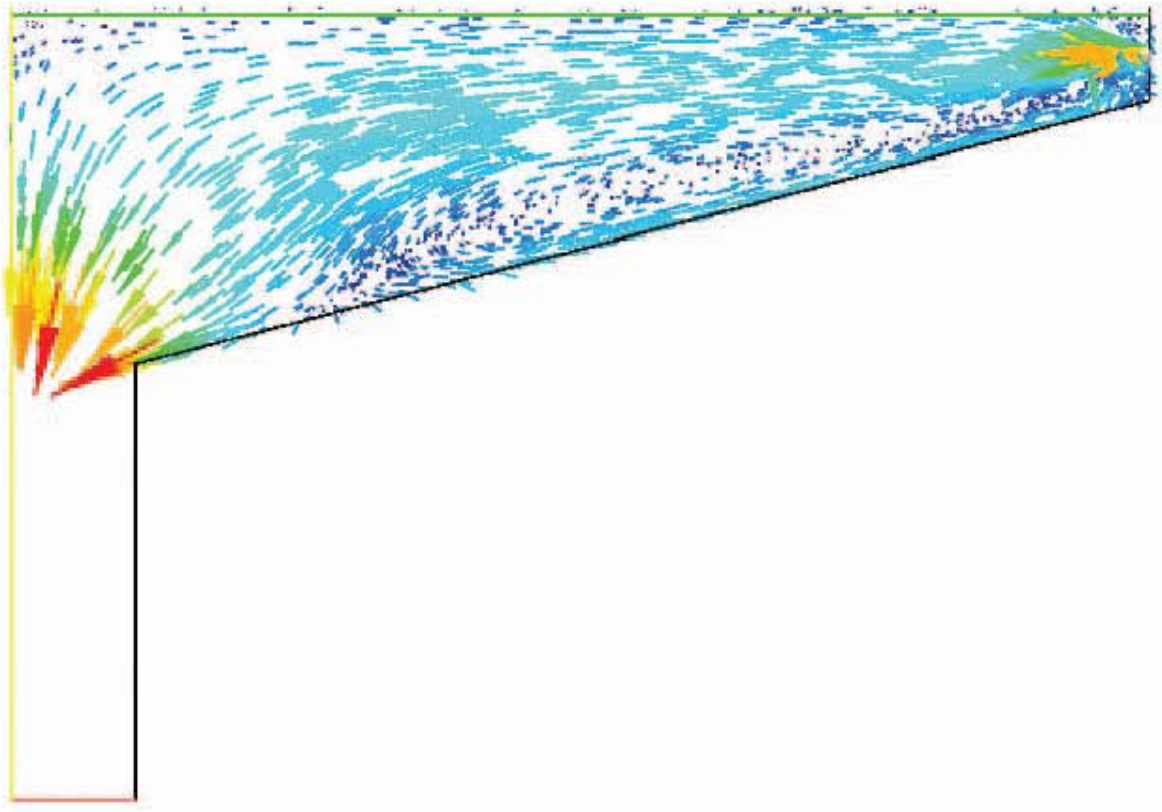

Figure 1.16 Predicted velocity profile for an evaporator vessel with peripheral feed and a central outlet, Steindl and Ingram (1999)

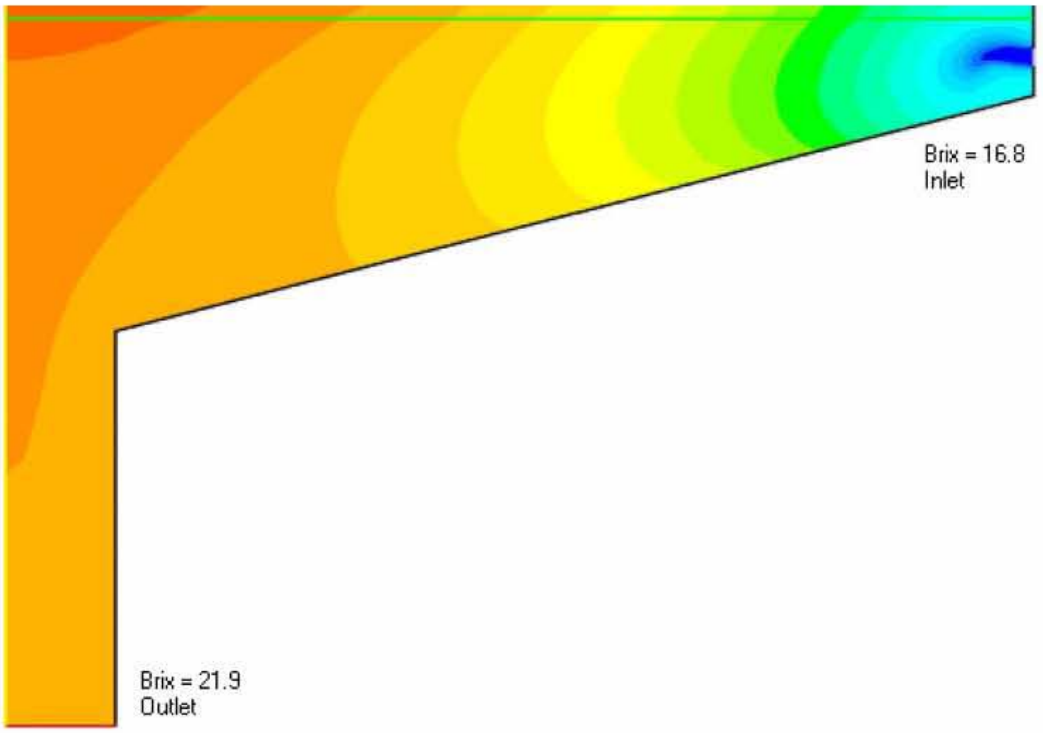

Figure 1.17 Predicted brix profile for an evaporator vessel with peripheral feed and a central outlet, Steindl and Ingram (1999)

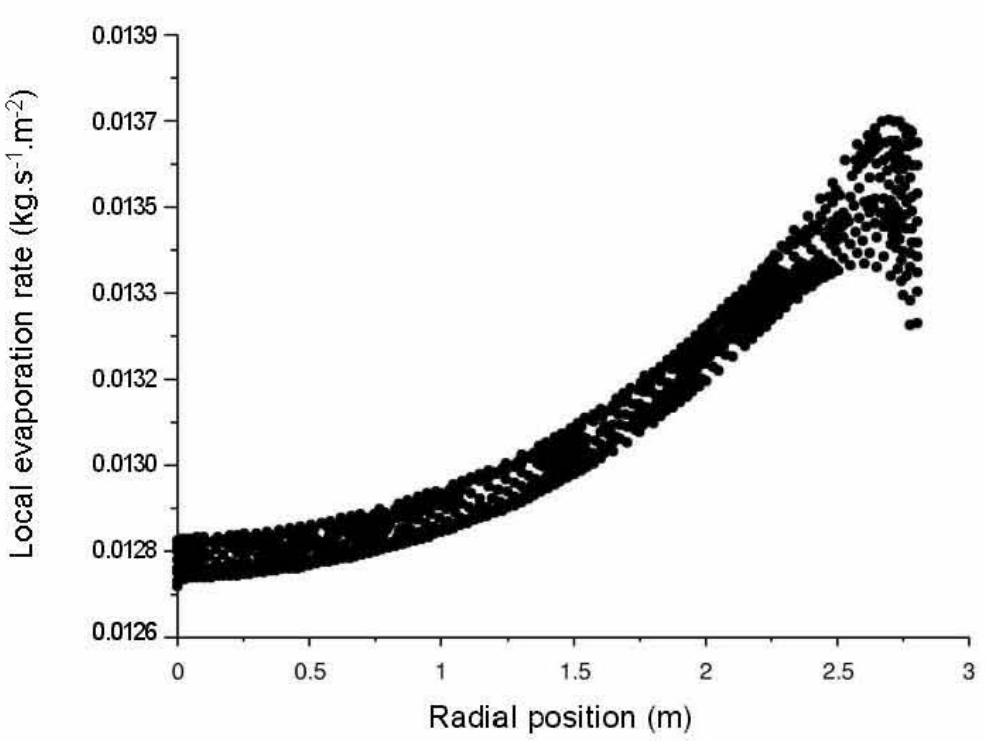

Figure 1.18 Predicted variation of the local evaporation rate with radial position for an evaporator vessel with peripheral feed and a central outlet, Steindl and Ingram (1999)

1.5.2 Stephens

Stephens (2001) developed a numerical model of natural circulation in high-grade evaporative crystallisation (vacuum) pans using the commercial CFD package CFX. It was successful in predicting the natural circulation due to boiling in a two-dimensional model. The model of the massecuite flow did not include the effect of the tubes within the CFX model. Instead this effect was accounted for by using characteristic equations in the user FORTRAN section of the CFX code. An attempt was made to model the boiling process within the tube using CFX, but problems with large computer run times were reported, similar to Steindl and Ingram (1999).

The overall model was divided into two parts with the effect of the tubes was modelled using a separate FORTRAN code and the fluid flow in the remainder of the vessel being modelled using the CFX code. Given the fluid properties and the tube geometry as user inputs, the FORTRAN code calculated the pressure distribution along the length of the tube and interchanged the inlet and outlet boundary conditions with CFX. This interchange was continued in an iterative process until the solution converged to a pre-determined tolerance value.

Whilst some of the modelling techniques developed by Stephens (2001) may be applicable to the modelling of evaporators, the model itself is not considered directly applicable since the temperature driving forces in vacuum pans is significantly larger, the liquid level changes in a vacuum pans due to batch mode of operation, vacuum pans operate with a static fluid level above the top tube-plate, there is a well defined flow path in a vacuum pan due to the presence of a large central downtake, no crystallisation occurs inside evaporator vessels, the viscosity of the working fluid in vacuum pans is significantly higher than in evaporator vessels, and evaporators are typically made of smaller and longer stainless steel tubes than the shorter, larger diameter mild steel tubes used in vacuum pans.

1.5.3 Evaporator modelling

This literature survey has shown that very few previous attempts have been made at developing a CFD model, of any description, of a sugar mill evaporator. Since this is the case the remainder of this investigation will treat the area of research almost as a green field site. As such the scope of the study has been limited in order to achieve a useful outcome, albeit with limitations.

The heat and fluid flow inside the calandria section are considered to be of the greatest complexity and simplifying assumptions will be required. Modern CFD techniques are expected to be capable of predicting the fluid flow in the remainder of the vessel without simplification, this is true even though previous attempts, such as Steindl and Ingram (1999) have been simplified.

While the modelling work of Stephens (2001) is considered to be not directly relevant to this work, there may be scope to combine the ideas of Stephens (2001) and Steindl and Ingram (1999) in a way that will allow for the successful development of a CFD model of a sugar mill evaporator.

To date very little is known about the heat and fluid flows inside the calandria section of an evaporator. This problem is likely to require an extensive study to resolve completely. This is supported by the fact that previous attempts at developing a CFD model of a sugar mill evaporator have ignored the heat and fluid flows in the calandria. However, it is likely that a number of simplifying assumptions can be made to adequately account for the calandria section. This would allow the development of a CFD model of the entire vessel.

1.6 Summary

The evaporator station is an important process station of a sugar mill and typically uses 50% of the LP steam consumed by the factory. The ever-present push towards an increase in overall factory steam economy directs its focus on the use of vapour from the evaporator station to perform the heating duties normally performed by LP steam. Increasing the efficiency of the evaporator station will not reduce factory steam consumption directly, but will provide greater opportunity for vapour to be used in place of LP steam. Hence the indirect effect on the overall steam economy of the factory.

CFD modelling has emerged in recent times as a powerful tool for the design of equipment handling fluid flows. However, due to the complex nature of the process very few attempts have been made at modelling a sugar mill evaporator. Past modelling attempts have experienced very large computer run times and large memory requirements. Some of the modelling packages commercially available have also been shown to give incorrect results. Modelling results to date have demonstrated the usefulness of the CFD tool and have highlighted the need for CFD modelling to provide insight into the design process.

All CFD modelling work requires validation against factory measurements in order to obtain confidence in the predictions produced. A comprehensive validation process has

been missing from previous modelling attempts and some questionable factory measurement procedures have also been identified.

2. Objectives

Chapter 1 of this thesis highlighted the need to have a CFD model capable of predicting the fluid flow inside an evaporator and the potential engineering benefits that could be realised by analysing these flows. The literature review showed that very few attempts had been made to develop such a model and those models included a large number of simplifying assumptions. The most significant assumption in previous attempts is the neglect of the calandria section of the vessel. The calandria section is thought to have a significant influence on the flow field inside the vessel. As a result, the objectives of this investigation are:

- To develop a CFD model of a sugar mill evaporator capable of predicting the fluid and heat flows inside the entire vessel,
- To develop a CFD model of a sugar mill evaporator capable of predicting trends when geometry such as inlet and bottom cone geometry are changed,
- To develop a CFD model of a sugar mill evaporator capable of allowing for the presence of the vapour phase without specifically modelling it, through the use of lumped parameters,
- To gather data from factory vessels and compare with predictions from the CFD model developed herein, and
- To apply the CFD model developed herein to investigate potential performance improvements that may be realised by modifying the geometry of evaporator vessels.

3. Factory experiments

3.1 Introduction

A properly validated CFD model is necessary to provide reliable simulations of the flow of juice inside an evaporator vessel. The CFD model should predict the physics of the flow field inside an evaporator vessel in spite of the assumptions used to develop the model. As no suitable data exists in the literature, a series of experiments was carried out on the Proserpine #4 and the Farleigh #2 vessels during the 2002-crushing season. The data gathered included brix and temperature values at important points within the flow fields. The operating conditions of the vessels were also monitored, the measurements taken were headspace and calandria pressures, juice in and out flow rates, inlet and outlet juice brix and temperatures, and vapour flow rates.

The juice brix and juice flow rate data enabled mass balance calculations on the juice flow to be carried out; while the juice temperature, headspace pressure, calandria pressure and vapour flow rate data enabled a heat balance calculation to be carried out on the entire system.

3.2 The Proserpine #4 evaporator vessel

The Proserpine Mill runs a quadruple-effect (unit) evaporator set (Figure 3.1). The first and third effects have three vessels in parallel, the second has two vessels in parallel and the fourth effect has only one vessel. The de-superheater supplies LP steam to the calandria of the first effect vessels, normally at a pressure of between 130 and 180 kPa abs. The vapour side operation of the Proserpine Mill evaporator set runs all vessels on each effect in parallel, with the vapour outlets from the headspace of each effect being combined prior to connection to the calandria of each vessel on the next effect. The headspace pressure of the final effect vessel is controlled by a vacuum pump. The vacuum pump is connected to the condenser that receives the vapour flow from the headspace of the final-effect. The vacuum pump controls the headspace pressure in the final-effect to a set point of approximately 14 kPa abs. The headspace and calandria pressures in all of the intermediate vessels are allowed to equilibrate by themselves.

As shown in Figure 3.2, the juice side operation of the Proserpine Mill evaporator set runs all vessels on each effect in parallel, with all juice outlets being combined prior to connection to the inlets of the vessels of the subsequent effect.

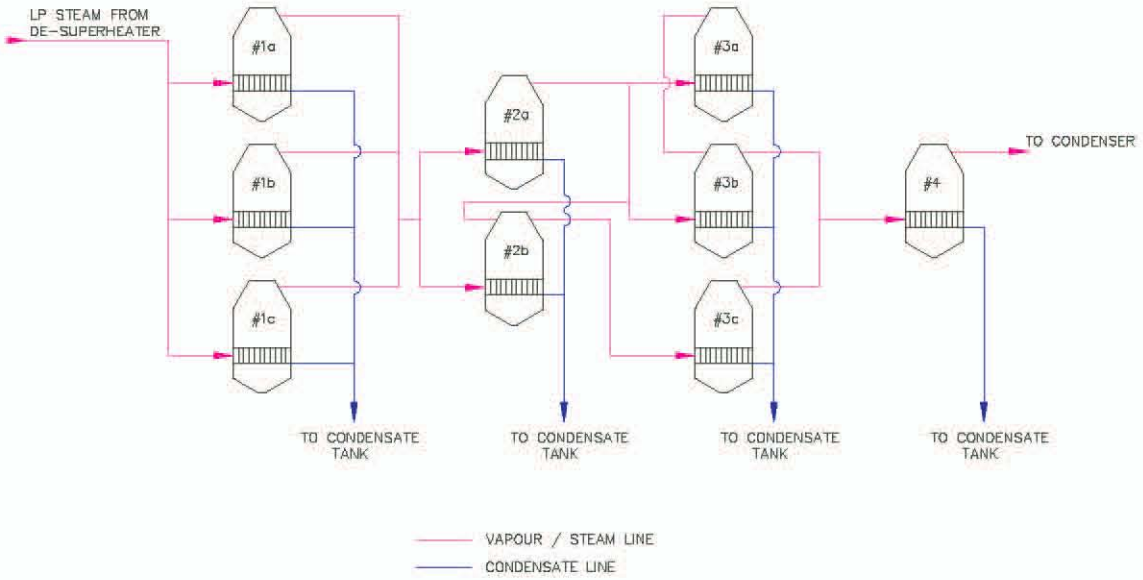

Figure 3.1 Schematic of the vapour side operation of the Proserpine Mill evaporator station

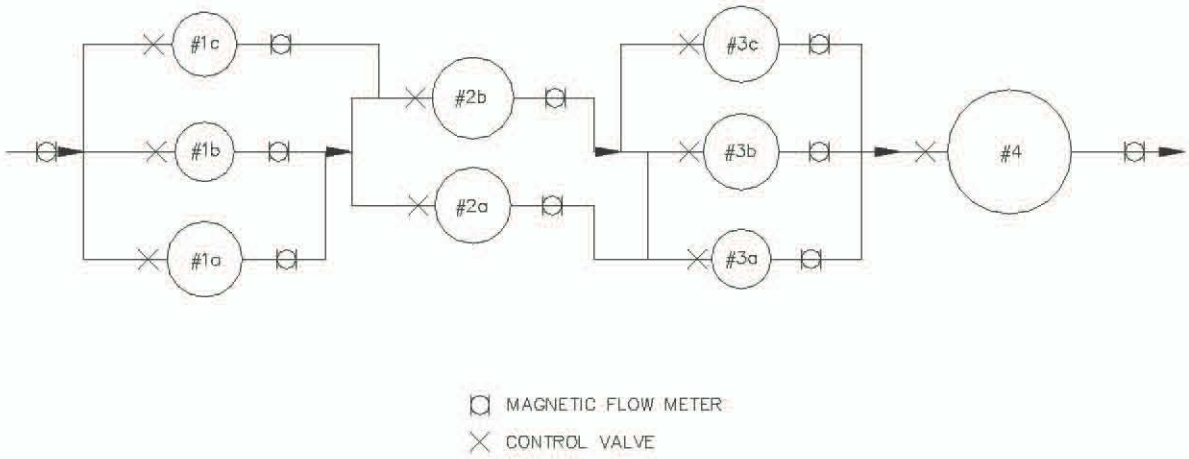

Figure 3.2 Schematic of the juice side operation of the Proserpine Mill evaporator station

Throttling the juice flow at the inlet controls the juice level inside each individual vessel. Throttling the juice flow at inlet to the #4 vessel also controls the juice brix at the outlet of the #4 vessel. The control system on the #4 vessel has a limit switch on the juice level within the vessel so that the juice level will not fall below the lower limit, even if the juice

brix at the outlet is below its set point. This system is to ensure that the vessel does not run dry.

Magnetic flow meters (Krohne, model IFS400) of 300 mm diameter, are used to measure the juice flow rate at the inlet and outlet of the #4 vessel. The flow rate measurements are not used for steady state control purposes, but only for start up, shut down, evaporator cleaning and monitoring the total juice flowing out of the final vessel.

The pressure difference between effects controls the vapour flow to the calandria of all vessels after the first effect and the condensate is allowed to flow under gravity into a storage tank. The condensate is then pumped from the storage tank to the cooling tower. Level switches inside the storage tank control the pump operation.

The Proserpine #4 vessel was chosen for this study because it has juice flow rate measurements on the inlet and the outlet. Use of the existing flow meters simplified the conduct of the experiments. The calandria also has a radial vapour feed system and is fitted with an array of 150 NB downtakes. The ability of the CFD model to accurately predict fluid flows in a vessel fitted with small downtakes was seen as a significant factor since all new vessels installed in recent years have been fitted with these downtakes.

3.3 The Farleigh #2 evaporator

The Farleigh Mill runs a quin-effect (unit) evaporator set (Figure 3.3). The first, second and fifth effects have only one vessel, the third effect has two vessels in parallel and the fourth effect has three vessels in parallel. LP steam is supplied to the calandria of the first-effect vessel from the exhaust of the mill and power station steam turbines, normally at a pressure of between 130 and 160 kPa abs. The vapour side operation of the Farleigh Mill evaporator set runs all vessels on each effect in parallel, with the vapour outlets from the headspace of each effect being combined prior to connection to the calandria of each vessel on the next effect. The headspace pressure of the final effect is controlled by a vacuum pump. The vacuum pump is connected to the condenser that receives vapour from the headspace of the final effect. The vacuum pump controls the headspace pressure in the final effect to a set point of approximately 16 kPa abs. The headspace and calandria pressures in all of the intermediate vessels are allowed to equilibrate to a constant value.

The Farleigh #2 vessel was chosen for this study because its operating pressures in the calandria and the headspace are significantly higher and the juice brix is significantly lower than the corresponding conditions inside the Proserpine #4 vessel. Data gathered from the

two vessels would be significantly different and would allow for a single CFD model to be developed which is capable of predicting flows under a wide range of operating conditions. The Farleigh #2 vessel also has no small downtakes fitted to the calandria; again this is different from the Proserpine #4 vessel. The Farleigh #1 was also considered for this study because it meets all of these criteria. However, the juice at the inlet of the Farleigh #1 vessel is sometimes at a temperature that is significantly lower than its saturation temperature. This forces the vessel to perform a large amount of sensible heating. The operating conditions of the Farleigh #2 vessel are very similar to those of the Farleigh #1 vessel but the data will not contain the complication of having sub-cooled juice at the inlet.

As shown in Figure 3.4, the juice side operation of the Farleigh Mill evaporator set does not run all vessels in parallel, for those effects containing multiple vessels. The outlet of the #3a vessel is connected to both the inlet of the #4b and #4c vessels, while the outlet of the #3b vessel is connected directly to the inlet of the #4a vessel. The outlets of the three fourth-effect vessels are joined prior to being connected to the inlet of the fifth-effect vessel.

Throttling the juice flow at inlet controls the juice level inside each individual vessel. There is no other control system on the Farleigh #2 vessel. Juice flow rates at the inlets and outlet of the vessels are not measured in the Farleigh evaporator station.

The pressure difference between effects controls the vapour flow to the calandria of the #2 and the condensate is allowed to flow under gravity to a pump. Unlike the set-up at Proserpine Mill, there is no intermediate storage tank between the vessel and the condensate pump.

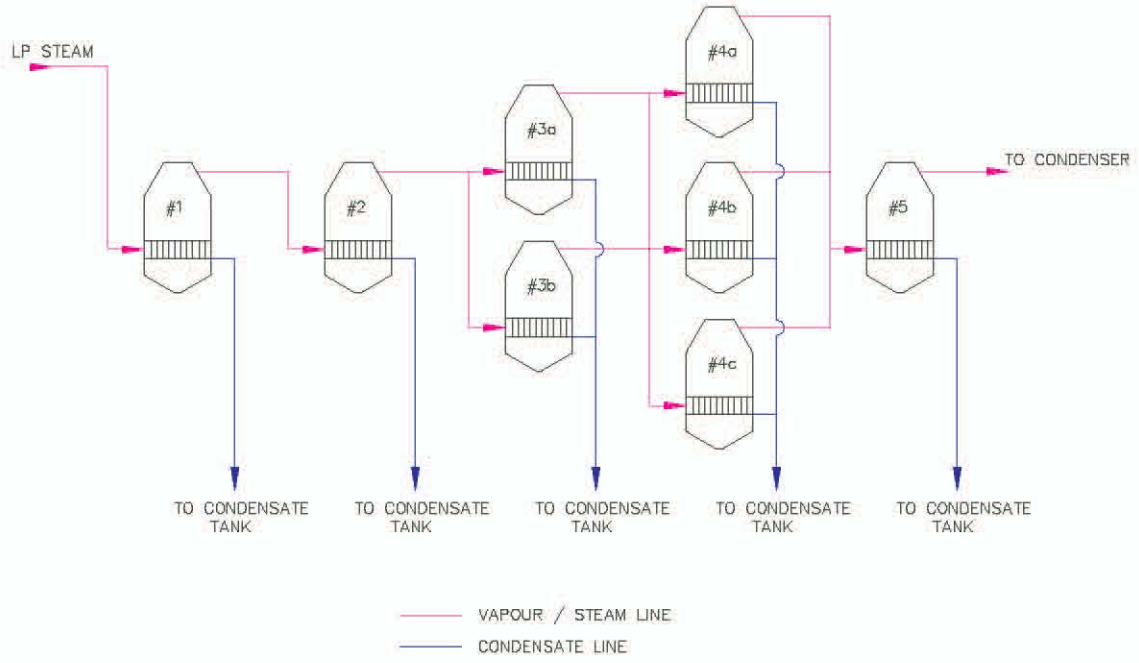

Figure 3.3 Schematic of the vapour side operation of the Farleigh Mill evaporator station

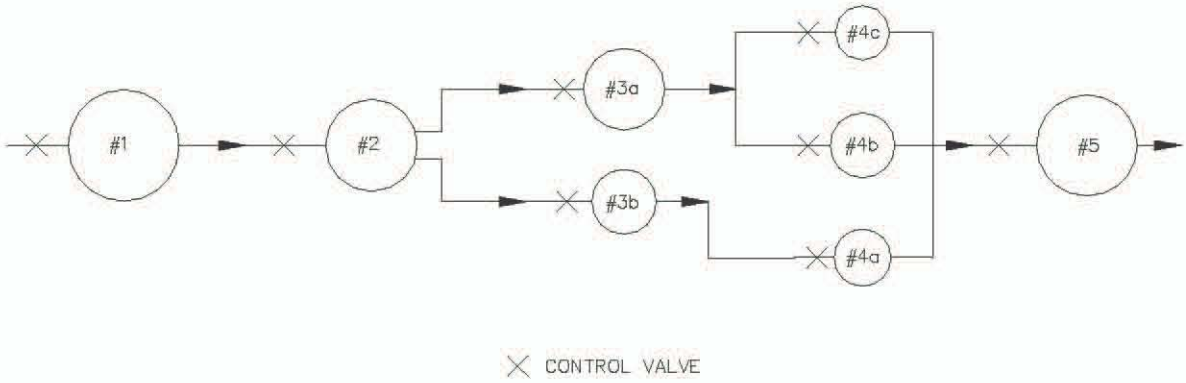

Figure 3.4 Schematic of the juice side operation of the Farleigh Mill evaporator station

3.4 Experimental equipment

Three tapping points were installed into the bottom of the Farleigh #2 and the Proserpine #4 vessels. Figure 3.5 and Figure 3.6 show the locations of these tapping points, in relation to the juice inlets and juice outlets, when viewed from above. The location of the tapping points was chosen because they approximately follow the expected flow path of the juice from inlet to outlet. The location of the tapping points in the Farleigh #2 vessel was limited

by external obstructions and are therefore not as close to the ideal flow path as the Proserpine #4 vessel.

At the time of installation the juice brix was expected to gradually increase as the fluid flowed from inlet, past points A, B and C then to the outlet. It was believed at the time that this would provide data with an even variation in brix.

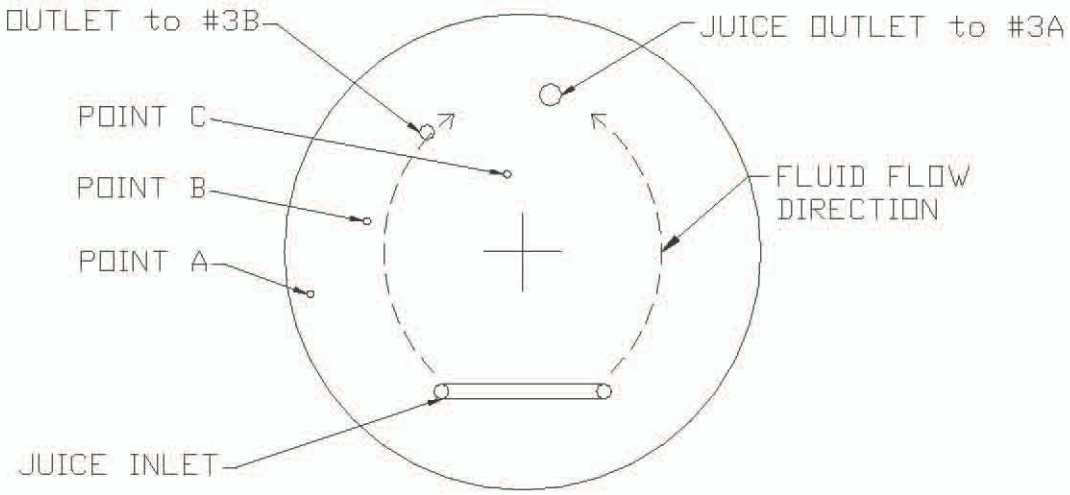

Figure 3.5 Location of tapping points installed in the bottom of the Farleigh #2 vessel when viewed from above

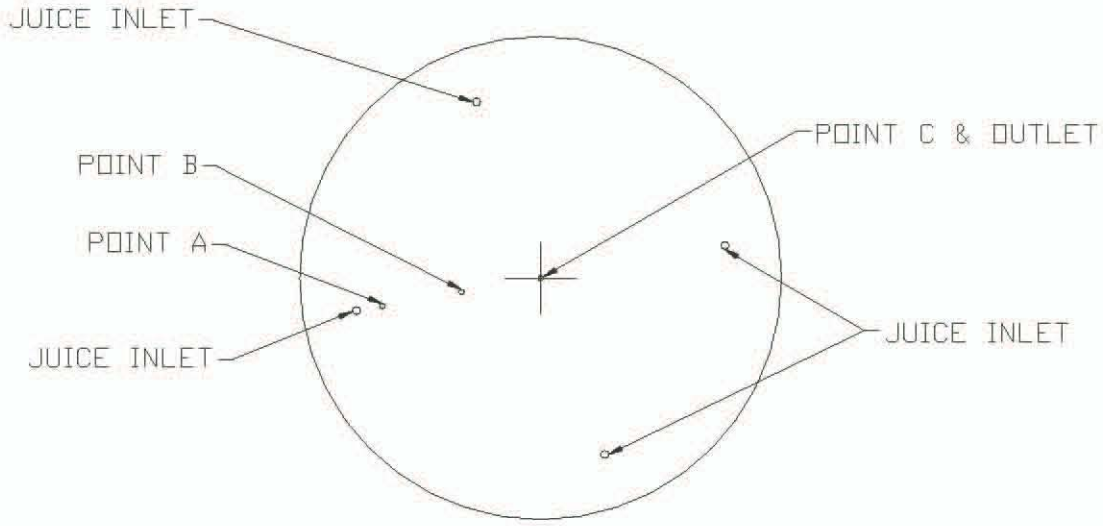

Figure 3.6 Location of tapping points installed in the bottom of the Proserpine #4 vessel when viewed from above

A sampling probe was inserted through a gland at each of the tapping points. The end of the sampling probes could be moved up and down, in the vertical direction, allowing samples and measurements to be taken at different distances above and below the bottom tube-plate. Using the bottom tube-plate as a datum, the vertical height of the sampling probe is expressed as –XX mm below the bottom tube-plate and +XX mm above the bottom tube-plate (ie. inside the heating tubes). Most of the sampling was done in the juice space below the bottom tube-plate but a small number of tests were conducted where the probes were inserted into the calandria tubes. Figure 3.7 shows a typical set up for the sampling probes when inserted into a vessel. Figure 3.8 is a photograph of one of the sampling probes showing the moveable gland that allows the probe to be positioned at different distances below the calandria.

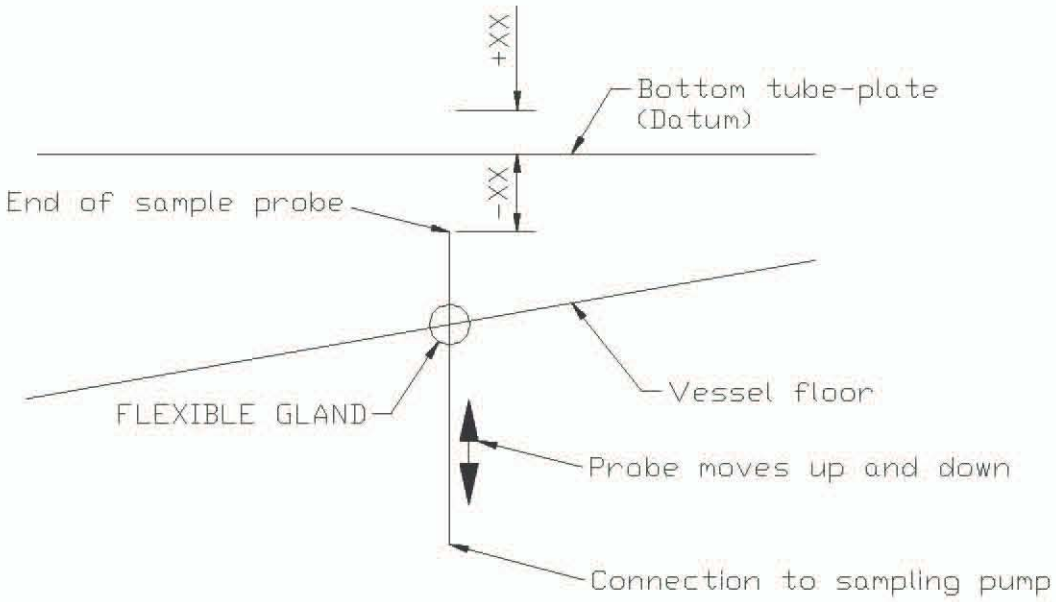

Figure 3.7 A side view of a sample probe positioned inside a vessel

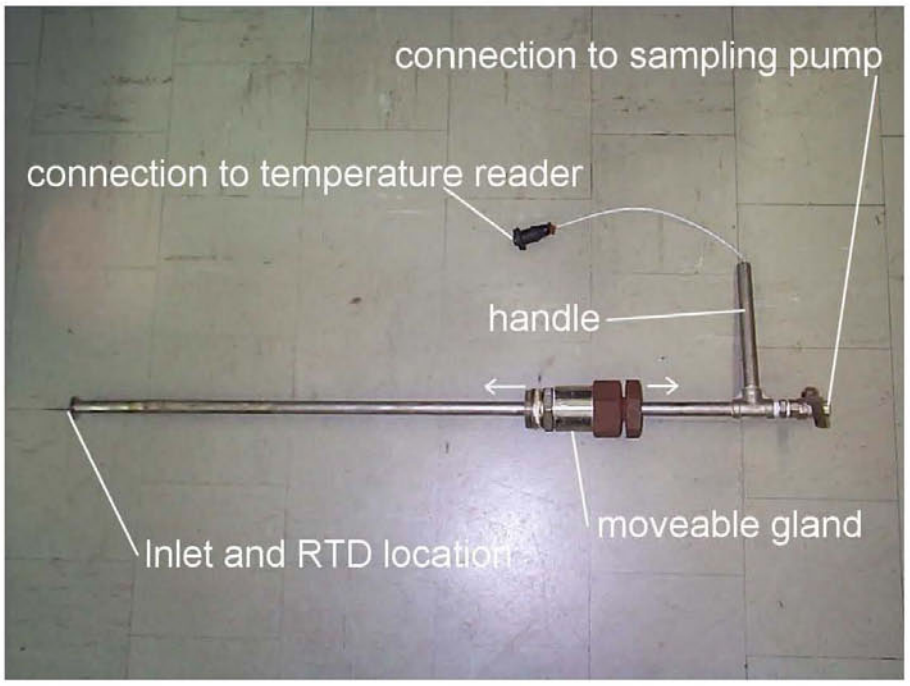

Figure 3.8 Photograph of a sampling probe

Four tests were conducted on the Proserpine #4 vessel and six tests were conducted on the Farleigh #2 vessel. Table 3.1 and Table 3.2 show the vertical locations of the sampling probes for each of the tests conducted. Refer to Figure 3.5 and Figure 3.6 for the locations of the sampling points in the horizontal plane.

Table 3.1 Sampling probe vertical locations for tests conducted on the Proserpine #4 vessel

Test no.	Probe location point A (mm)	Probe location point B (mm)	Probe location point C (mm)
1	0	+136	-408
2	0	-64	-608
3	-200	-64	-608
4	-200	-264	-808

Table 3.2 Sampling probe vertical locations for tests conducted on the Farleigh #2 vessel

Test no.	Probe location point A (mm)	Probe location point B (mm)	Probe location point C (mm)
1	+387	+248	n/a
2	+187	+48	0
3	+187	0	0
4	+187	-200	-200
5	-13	-20	0
6	-13	-220	-200

A small peristaltic pump was connected to the inlet, outlet and to each sample probe to pump out a small amount of juice at each point. A cooling coil was connected to the discharge of the pump. The cooling coils were used to prevent flashing of the juice during sampling and thus prevent changes in the juice brix. The pumps produced a continuous flow of juice that could then be sampled and analysed at a later date in the laboratory. The juice flow rate through the sampling pumps was considered to be small enough so as not to disturb the juice flow patterns inside the evaporator.

The temperature sensors placed inside the sampling probes and in the inlet and outlet pipes were connected to a data logger and the readings were recorded at a 30-second frequency. The temperature sensors were calibrated at three different temperatures (0°C, 60°C and 100°C) prior to installation. The temperature readings were within ±0.5°C of the calibration instrument. The juice temperature at the outlet of the Proserpine #4 vessel was not recorded due to equipment failure. However, a heat balance calculation could still be performed using the juice temperature at inlet.

A Druck, model DPI 705, hand-held pressure meter, with an accuracy of ±0.02 kPa, was used to measure all headspace and calandria pressures.

The condensate flow rates were measured using an ultrasonic flow meter on the discharge of the condensate pump and the readings were recorded at a 30-second frequency. The flow meter was a Panametrics, model PT868-R, portable liquid flow meter. When used for water the accuracy of the flow meter is expected to be better than $\pm 2.5 m^3 \cdot h^{-1}$ (less than 1% of the largest expected condensate flow).

The juice flow rate at the inlet to the Farleigh #2 vessel was measured using an ultrasonic flow meter identical to the meter used on the condensate flow. The flow meter was not calibrated for sugar solutions and the accuracy of these reading is expected to be less precise than the readings obtained for the condensate flows. However, the instrument's internal software contains an allowance for the fluid viscosity and the speed of sound within the fluid. Both of these are known fluid properties that can be calculated using both the brix and temperature of the juice. This was done immediately prior to the beginning of each test and was assumed to be the same for the duration of the test.

The juice flow rate at the inlet to the Proserpine #4 vessel was measured using the Mill's magnetic flow meter and the readings were recorded at a 30-second frequency. The accuracy of the flow meters was checked against a reading obtained using the ultrasonic

flow meter in the same procedure that was used for the Farleigh #2 vessel. The magnetic flow meter was found to have an average bias of –25 $m^3 \cdot h^{-1}$, when logged over a 6-minute time period. A correction was applied to the readings to correct the bias.

An attempt was made to measure the juice flow rate at the outlet of the Proserpine #4 vessel using the Mill's magnetic flow meter. However, the flow meter was found to be malfunctioning and no readings from this instrument were possible. No attempt was made to measure the juice flow rate at the outlet(s) of the Farleigh #2 vessel since the Mill does not have flow meters currently installed and the additional effort required to measure these data was seen as unnecessary. The unavailability of these data were seen as a small disadvantage since it prevented the mass and energy balance calculations to be performed using three independent methods rather than just two methods. Performing the calculations three times allows the accuracy of the experimental data to be evaluated more accurately than when the calculations are performed twice. While the ability to evaluate accuracy is reduced, the available data does not prevent CFD model comparison.

3.5 Experimental procedure

Juice samples were collected from the sample pumps at a 3-minute frequency. Although higher frequency sampling was preferred, it was found that 3 minutes was the shortest amount of time required to physically collect the juice samples from the sampling pumps. Each of the juice samples was sealed immediately after collection to prevent any flashing or evaporation that may occur to preserve the juice brix. Although each sampling pump was fitted with a cooling coil on its discharge port the juice temperature at exit was approximately 40°C for the Proserpine #4 tests and between 45 and 50°C for the Farleigh #2 tests. It was believed that at these temperatures it was possible for the juice to lose sufficient water and have a significant influence on the brix of the sample. Accordingly, great care was taken to avoid flashing and evaporation.

The juice samples were then taken to the laboratory and cooled to 20°C in a cold-water bath before being analysed for brix using a standard laboratory method and a Bellingham Stanley, RFM320 refractometer with an accuracy of ±0.05 units of brix.

The headspace and calandria pressure measurements were measured at a 3-minute frequency. As with the juice sampling, 3 minutes was found to be the shortest amount of time required to physically collect the data.

The stable liquid level above the top tube-plate (dynamic head) was measured manually against graduations marked on the sight glass, at a 3-minute frequency. The dynamic head was not expected to change during the tests but was monitored to eliminate uncertainty. In all cases the dynamic head was constant with only negligible variations during each test. However, the dynamic head did vary significantly between tests.

Each test was conducted over a 30-minute period since it was considered that 30 minutes was a long enough time to account for any operational fluctuations. Due to the very fast and random nature of the short-term fluctuations in the system, data logged once every three minutes would be suitable for performing reasonable heat and mass balances. Data points recorded once every three minutes for a 30-minute period (i.e. 11 readings) was believed to be the smallest number of readings that would still provide a statistically significant average and standard deviation. These average and standard deviation values are displayed in Table 3.3 and Table 3.4.

The long-term operational fluctuations were unable to be controlled. Each 30-minute period of data collected was examined to ensure that the vessel was operating under stable operating conditions for the duration of the test. It was discovered that in most cases the long-term fluctuations in operating conditions were of time-scales sufficiently long enough that suitable data could be gathered in a 30-minute period. On the rare occasion where the data was found to be unsuitable, the data was discarded and the experiment was repeated.

Figure 3.9 is a plot showing the juice flow rate at the inlet to the Proserpine #4 vessel for one of the tests and is typical of the flow rate data gathered from both the Proserpine #4 and the Farleigh #2 vessels. It shows instantaneous flow rate measurement has significant short-term fluctuations but relatively small long-term fluctuations. This plot demonstrates the ability of the experimental method described above to account for the short-term and long-term fluctuations in the system and to provide a useful data for heat and mass balance calculations. Figure 3.10 shows that the headspace and calandria pressures have significantly smaller short-term fluctuations than the juice flow rate.

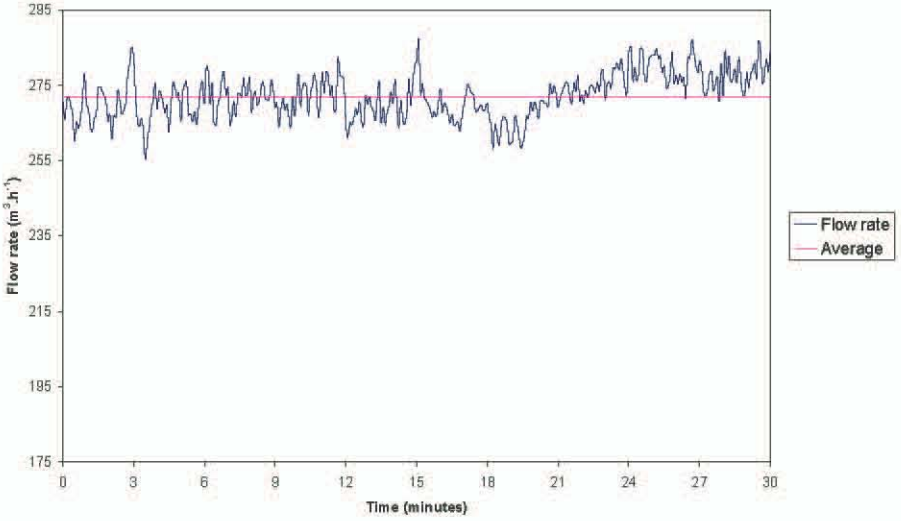

Figure 3.9 Plot of juice flow rate at the inlet to the Proserpine #4 vessel for test no. 3

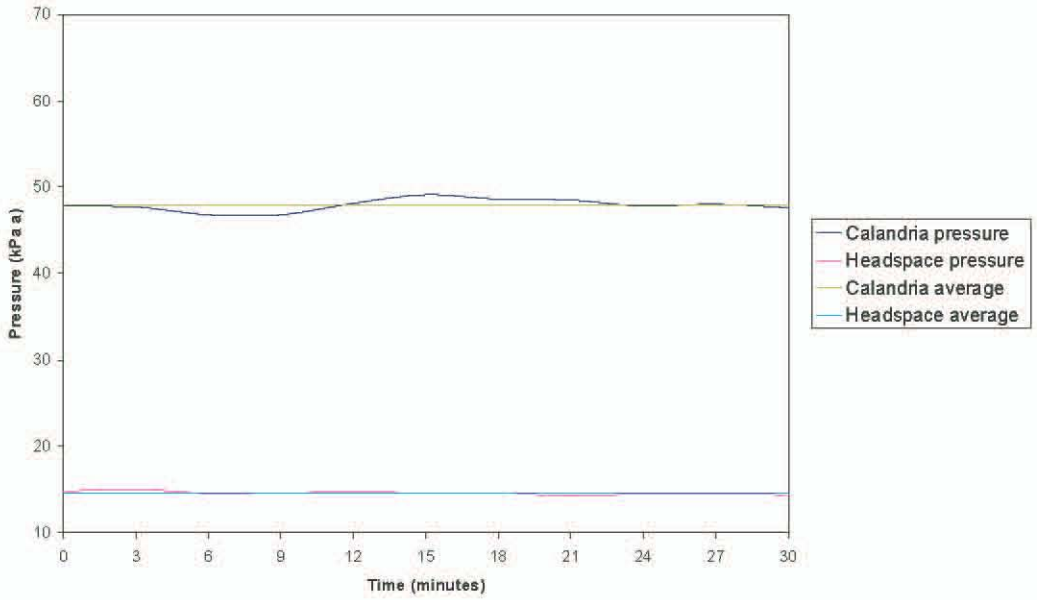

Figure 3.10 Plot of headspace and calandria pressures in the Proserpine #4 vessel for test no. 3

For the Proserpine #4 vessel tests no. 1 and 2 were conducted before the vessel was cleaned and tests no. 3 and 4 were conducted after the vessel was cleaned. For the Farleigh #2 vessel tests no. 1 to 4 were conducted before the vessel was cleaned and tests no. 5 and 6 were conducted after the vessel was cleaned. This procedure was adopted in order to gain the widest possible variation in processing conditions, i.e., when fouling of the heating

tubes was at worst and best conditions. This gives the best indication of the magnitude of any changes in processing conditions experienced during normal operation.

3.6 Experimental results

All of the data logged for the four tests conducted on the Proserpine #4 vessel are shown in Table 3.3. All of the data logged for the six tests conducted on the Farleigh #2 vessel are shown in Table 3.4. In all cases the average value is reported along with the corresponding standard deviation.

Table 3.3 Summary of data from the Proserpine #4 vessel

Test no.		**1**	**2**	**3**	**4**
Before / after clean		before	before	after	after
Juice flow rate at inlet ($m^3 \cdot h^{-1}$)	average	258.2	267.7	272.1	273.1
	standard deviation	12.6	17.7	6.0	8.0
Calandria pressure (kPa abs)	average	62.3	64.1	47.9	47.4
	standard deviation	0.8	4.0	0.7	1.2
Headspace pressure (kPa abs)	average	13.7	13.8	14.6	14.8
	standard deviation	0.3	0.4	0.2	0.5
Condensate flow rate ($m^3 \cdot h^{-1}$)	average	136.3	135.6	141.6	138.2
	standard deviation	3.2	4.8	2.5	2.6
Dynamic head (mm)	average	300	300	310	310
	standard deviation	0.0	0.0	0.0	0.0
Juice temperature at inlet (°C)	average	87.8	88.9	81.3	81.3
	standard deviation	0.3	1.4	0.7	0.5
Juice temperature at point A (°C)	average	55.1	55.5	57.6	58.0
	standard deviation	0.2	0.4	0.2	0.5
Juice temperature at point B (°C)	average	55.0	55.1	56.0	57.3
	standard deviation	0.2	0.3	0.3	0.5
Juice temperature at point C (°C)	average	57.0	57.3	58.8	58.8
	standard deviation	0.2	0.3	0.2	0.5
Juice brix at inlet (%-wt)	average	35.6	36.3	37.7	38.1
	standard deviation	0.6	0.9	0.7	0.3
Juice brix at outlet (%-wt)	average	63.1	63.7	67.5	67.1
	standard deviation	0.6	0.5	0.5	0.4
Juice brix at point A (%-wt)	average	63.5	64.4	68.5	68.1
	standard deviation	0.6	0.4	0.2	0.2
Juice brix at point B (%-wt)	average	65.0	65.7	72.9	69.1
	standard deviation	0.6	0.5	0.4	0.6
Juice brix at point C (%-wt)	average	63.6	64.5	67.1	66.7
	standard deviation	0.5	0.5	0.2	0.3

Table 3.4 Summary of data from the Farleigh #2 vessel

Test no.		**1**	**2**	**3**	**4**	**5**	**6**
Before / after clean		before	before	before	before	after	after
Juice flow rate at inlet ($m^3 \cdot h^{-1}$)	average	365.3	315.3	262.8	277.7	344.9	341.0
	standard deviation	27.6	28.0	49.5	70.4	34.2	22.4
Calandria pressure (kPa abs)	average	125.9	125.5	103.2	106.8	111.7	111.8
	standard deviation	1.2	0.3	6.5	7.7	0.4	0.4
Headspace pressure (kPa abs)	average	98.0	97.7	81.7	82.6	87.4	88.3
	standard deviation	0.6	0.3	5.8	5.5	0.5	0.4
Condensate flow rate ($m^3 \cdot h^{-1}$)	average	56.6	57.1	36.8	36.1	50.6	51.3
	standard deviation	1.9	3.4	6.1	7.5	2.8	1.0
Dynamic head (mm)	average	571	530	443	450	424	440
	standard deviation	28.4	0.0	107	109	12.1	0.0
Juice temperature at inlet (°C)	average	100.8	100.9	100.4	99.8	95.2	101.0
	standard deviation	0.7	0.4	1.4	1.7	3.8	0.2
Juice temperature at outlet#3a (°C)	average	99.3	99.3	93.2	94.5	n/a	n/a
	standard deviation	0.2	0.1	1.8	1.3	n/a	n/a
Juice temperature at outlet#3b (°C)	average	99.0	99.3	92.1	93.3	92.6	93.7
	standard deviation	0.3	0.2	2.0	1.5	1.7	0.6
Juice temperature at point A (°C)	average	98.4	98.5	91.9	93.3	92.2	95.2
	standard deviation	0.2	0.1	1.8	1.6	1.2	0.3
Juice temperature at point B (°C)	average	97.3	97.2	91.3	92.6	92.4	94.0
	standard deviation	0.3	0.1	1.6	1.7	1.0	0.3
Juice temperature at point C (°C)	average	n/a	95.0	90.2	92.3	93.1	94.7
	standard deviation	n/a	0.7	1.1	1.4	0.9	0.3
Juice brix at inlet (%-wt)	average	22.5	21.7	23.9	22.7	22.1	22.4
	standard deviation	0.3	0.4	0.5	1.5	0.3	0.4
Juice brix at outlet to #3a (%-wt)	average	26.3	25.4	27.8	27.0	25.9	26.3
	standard deviation	0.5	0.3	0.7	1.1	0.3	0.5
Juice brix at outlet to #3b (%-wt)	average	26.8	25.9	28.2	27.2	26.6	26.9
	standard deviation	0.6	0.3	1.1	1.4	0.3	0.4
Juice brix at point A (%-wt)	average	28.3	27.1	n/a	n/a	n/a	n/a
	standard deviation	1.0	0.3	n/a	n/a	n/a	n/a
Juice brix at point B (%-wt)	average	27.4	26.4	28.7	27.5	26.9	27.2
	standard deviation	0.6	0.2	1.3	1.3	0.4	0.4
Juice brix at point C (%-wt)	average	n/a	n/a	27.5	26.4	26.0	26.4
	standard deviation	n/a	n/a	0.8	1.2	0.2	0.4

The data from both the Proserpine #4 vessel and the Farleigh #2 vessel show that the juice brix at points A, B, and C are all very close to the juice brix at the outlet of the vessel. This result was not expected since the locations of the tapping points approximately follow the juice flow from the inlet towards the outlet. These data indicate that the juice flowing in the region below the calandria experiences very little variation in brix.

Table 3.3 shows a significant reduction in the calandria pressure and a slight increase in the headspace pressure in the Proserpine #4 vessel after it was cleaned. This is a normal

reaction to the improved heat transfer achieved by cleaning the heating tubes. The same trend is not obvious in the Farleigh #2 vessel. However, tests 3 and 4 conducted on the Farleigh #2 vessel were at significantly reduced flow rate that in turn caused a reduction in the operating pressures. If tests 3 and 4 are removed from the data table then the reduction in calandria pressure becomes apparent but a reduction in headspace pressure is also apparent.

The quantity of heat flowing through the calandria can be calculated in two ways, by calculating the quantity of heat released by the condensing steam or the quantity of heat required to evaporate the vapour produced. If the data is accurate then the difference between these two quantities is accounted for by thermal losses through the vessel walls and a change in sensible heat due to the different pressures. The heat released by condensation (Q_c) and the heat required for evaporation (Q_e) are calculated as follows:

$$Q_e = h_{fg}\,\dot{m}_e \qquad (3.1)$$

$$Q_c = h_{fg}\,\dot{m}_c \qquad (3.2)$$

The magnitude of h_{fg} as used in equations (3.1) and (3.2) is determined from steam tables using the headspace pressure for Q_e and the calandria pressure for Q_c.

The results of the heat balance calculations for the Proserpine #4 and the Farleigh #2 vessels are in Table 3.5 and Table 3.6 respectively. In all cases the difference between the two calculations is displayed as the percentage of the value calculated from condensation. This value was used as the reference since it is less likely to contain significant errors. A more comprehensive example of the heat and mass balance calculations is at appendix B.

Table 3.5 Results of heat balance calculations on the Proserpine #4 vessel

Test No.	1	2	3	4
Heat released by condensation (MW)	83.90	83.39	88.21	86.13
Heat required for evaporation (MW)	73.52	75.02	82.18	80.72
Difference between quantities (%)	-12.4	-10.0	-6.8	-6.3

Table 3.6 Results of heat balance calculations on the Farleigh #2 vessel

Test No.	1	2	3	4	5	6
Heat released by condensation (MW)	33.62	33.90	22.10	21.63	30.21	30.64
Heat required for evaporation (MW)	30.59	26.41	22.12	26.07	30.12	29.93
Difference between quantities (%)	-9.0	-22.1	+0.1	+20.5	-0.3	-2.3

The heat balance calculations on the Proserpine #4 data show reasonable agreement in all four tests conducted, with the largest error being –12.4%. The data from the Farleigh #2 vessel also shows close agreement for all cases except tests 2 and 4, with the largest error being –9.0%. For tests 2 and 4 the error is greater than 20% and the accuracy of the data gathered as part of these tests must be questioned.

3.7 Possible errors

The experimental program was implemented in the crushing season during the first year of the investigation. The data gathered from those experiments was found to be unsuitable for CFD model validation. All of the data from the first round of experiments was disregarded, the procedure was refined and the factory experiments were repeated in the crushing season during the second year of the investigation. Although the data displayed herein includes some errors, the accuracy was significantly improved from the first attempt.

The most significant source of error experienced in these experiments is the fluctuations in the operating conditions. All operating conditions (flow rates, juice brix at inlet, pressures and temperatures) vary from one minute to the next. This causes difficulties when gathering data to be used as boundary conditions for a CFD model and for comparison with model predictions. This is especially so since the model assumes the process is happening under steady state conditions. Short term fluctuations in juice and condensate flow rates were found to be up to plus and minus 10% of the averaged reading. This has a significant effect on the calculated heat transfer because it results in the proportional shift in the calculated heat transfer. It is for these reasons that the tests were conducted over a 30-minute period and the data were averaged. This averaging over time produced a close approximation to steady state conditions and proved to be repeatable.

When collecting samples of juice from the sampling pumps there is an inherent risk of contamination and of water evaporating from the juice, and therefore changing the brix, prior to measurement. Although every effort was taken to minimise these risks they are still a source of possible error and should be identified as such. It is believed that the error induced in the data displayed herein is negligible but it is almost impossible to quantify.

Greater difficulty was experienced obtaining a reading from the ultrasonic flow meter used to measure condensate flow rates from the condensate outlet line from the vessel. This is due to the presence of vapour in the flow. Placing the flow meter on the discharge line of the condensate pump was successful in obtaining a reading from the instrument due to the

increased pressure preventing any flashing of the condensate from occurring. This procedure will not induce any errors in the readings obtained since the mass inside the pipe is conserved; it merely changes from the vapour to the liquid phase. This was not seen as a disadvantage for this work, since only the long-term averaged data was used, but should be noted if these data are to be used for other applications or in other studies in the future.

The ultrasonic flow meter is not normally used to measure the flow rates of liquids such as juice. However, the meter can be adjusted according to the speed of sound in juice and its viscosity. These known fluid properties are a function of the juice brix and temperature. The temperature of the fluid was measured and a sample was taken, to determine brix, before the commencement of each test. This allowed the required fluid properties to be determined. However, this was done only once at the start of each test and was assumed to remain constant for the duration. Fluctuations in juice brix and temperature over time would therefore induce small errors in the flow rate measurements made by the flow meter.

The errors obtained with the magnetic flow meters on the juice inlet line to the Proserpine #4 vessel required significant effort to correct to ensure reliable data was gathered. This was done in a series of tests where the readings from the magnetic flow meter were checked against readings of the same flow rate using the ultrasonic flow meter. Each magnetic flow meter was checked individually. Although the comparison of individual data points in the short-term showed significant difference between the magnetic and the ultrasonic flow meter readings, the long-term averaged values were within acceptable limits, (less than 4% error). A heat balance performed on the vessel showed close agreement between the calculated values of heat flow through the calandria. This serves as additional evidence for the acceptance of the flow rate data and its use in subsequent calculations.

The results of the heat balance show that the difference between Q_1 and Q_2 is less than -12.4% for the Proserpine #4 vessel and less than -22.1% for the Farleigh #2 vessel. The magnitude of this difference should be approximately 4-5%, with the difference being explained by thermal losses through the walls of the vessel. However, the amount of thermal loss differs from vessel to vessel depending on the state of the insulation. In this case the insulation on the Farleigh #2 vessel was of reasonably poor quality and the difference is expected to be higher by a small amount. The difference should always be negative since the heat lost reduces the amount of evaporation. This is the case for the Proserpine #4 vessel but test #4 on the Farleigh #2 vessel shows a difference on +20.5%.

This is likely to be caused by errors in juice flow rate measurement and the data gathered from this test should be used cautiously.

3.8 Discussion of experimental results

3.8.1 Inlet and outlet juice temperatures

The juice temperature at the inlet of the vessel was calculated in order to confirm the accuracy of the measured data. The inlet juice temperature was calculated as the saturation temperature of the vapour at headspace pressure plus the boiling point elevation of the juice at the given brix. Table 3.7 shows the comparisons of measured and calculated data for the four tests performed on the Proserpine #4 vessel and Table 3.8 shows the comparisons for the six tests performed on the Farleigh #2 vessel. The values are within acceptable differences of each other, except for the values of the juice temperature at the inlet to the Farleigh #2 vessel. For test numbers 1, 2 and 5 the differences are significant. This is likely caused by the location of the temperature sensor in the inlet line. The sensor was inserted horizontally, through the sidewall of the inlet line, perpendicular to the fluid flow, but was not long enough to reach the centre of the pipe. The pipe was not insulated and the thermal losses were expected to be significant, thus causing a lower than actual temperature measurement.

Table 3.7 Estimated and measured juice temperatures at the inlet of the Proserpine #4 vessel

Test no.	**1**	**2**	**3**	**4**
Estimated juice temp at inlet (°C)	88.0	88.7	81.4	81.1
Measured juice temp at inlet (°C)	87.8	88.9	81.3	81.3
Difference in juice temps at inlet (°C)	-0.2	+0.2	-0.1	+0.2

Table 3.8 Estimated and measured juice temperatures at the inlet of the Farleigh #2 vessel

Test no.	1	2	3	4	5	6
Estimated juice temp at inlet (°C)	106.7	106.6	101.1	102.0	103.3	103.3
Measured juice temp at inlet (°C)	100.8	100.9	100.4	99.8	95.2	101.0
Difference in juice temps at inlet (°C)	-5.9	-5.7	-0.7	-2.2	-8.1	-2.4
Estimated juice temp at outlet#3a (°C)	99.7	99.6	94.8	95.1	n/a	n/a
Measured juice temp at outlet#3a (°C)	99.3	99.3	93.2	94.5	n/a	n/a
Difference in juice temps at outlet#3a (°C)	-0.4	-0.3	-1.6	-0.6	n/a	n/a
Estimated juice temp at outlet#3b (°C)	99.8	99.6	94.8	95.1	96.6	96.9
Measured juice temp at outlet#3b (°C)	99.0	99.3	92.1	93.3	92.6	93.7
Difference in juice temps at outlet#3b (°C)	-0.8	-0.3	-2.7	-1.8	-4.0	-3.2

3.8.2 Temperature distribution

Table 3.3 and Table 3.4 show that in all cases the juice temperatures at points A to C are all reasonably similar in magnitude. The absence of hot or cold spots within the juice would indicate reasonably uniform heat distribution within the flow field.

Table 3.3 shows that for all four tests conducted on the Proserpine #4 vessel, the temperature at point C is higher than the temperatures at points A and B. Although the difference is small it shows a consistent trend and would tend to indicate that the high brix juice in that region is being mixed with lower brix juice short-circuiting from the inlet, prior to exiting the vessel. This indicates poor circulation and heat transfer performance inside the Proserpine #4 vessel. Table 3.4 does not show the same trend occurring in the Farleigh #2 vessel.

3.8.3 Brix distribution

Table 3.3 and Table 3.4 show that for the tests conducted on both vessels, the juice brix at points A to C in a majority of tests are very close to the juice brix at the outlet and in some cases are higher. This is in spite of the tapping points being distributed approximately along the predominant fluid flow direction; refer to Figure 3.5 and Figure 3.6 for the location of the tapping points. This suggests that those heating tubes immediately above the juice inlet are the only tubes exposed to lower brix juice (comparable in magnitude to the inlet brix), all others are exposed to higher brix material (comparable to the outlet brix). This is detrimental to performance since a majority of the heating tubes are exposed to juice at a higher brix, and therefore viscosity, making it harder to transfer heat into the juice and so reducing the heat transfer performance of the vessel.

3.9 Data used for CFD modelling

All of the data tables displayed so far in this chapter have been comprehensive and useful for engineering purposes however; not all of these data are used for CFD modelling purposes. Those data used for the CFD modelling are summarised below.

Table 3.9 and Table 3.10 provide a summary of the vertical locations of the sampling points for the tests conducted on the Proserpine #4 and the Farleigh #2 vessels respectively. The location of these sampling points will be used to compare with the model predictions at corresponding locations. These data have been repeated in these tables to aid clarity.

Table 3.9 Summary of vertical locations of the sampling points used for the Proserpine #4 vessel

Test no.	Probe location point A (mm)	Probe location point B (mm)	Probe location point C (mm)
1	0	+136	-408
2	0	-64	-608
3	-200	-64	-608
4	-200	-264	-808

Table 3.10 Summary of vertical locations of the sampling points used for the Farleigh #2 vessel

Test no.	Probe location point A (mm)	Probe location point B (mm)	Probe location point C (mm)
1	+387	+248	n/a
2	+187	+48	n/a
3	+187	0	0
4	+187	-200	-200
5	-13	-20	0
6	-13	-220	-200

Table 3.11 and Table 3.12 provide a summary of the data used to set boundary conditions within the CFD models of the Proserpine #4 and the Farleigh #2 vessels respectively. These data were input into the model and were not predicted. At this point is should be noted that the condensate flow rate data were used to calculate the total quantity of heat flowing through the calandria of the vessel. This was initially set as a boundary condition for validation purposes, but was eventually replaced by an equation to predict this quantity. The details of this procedure are discussed in detail in later chapters of this thesis.

Table 3.11 Summary of data used as boundary conditions for the CFD model of the Proserpine #4 vessel

Test no.	**1**	**2**	**3**	**4**
Before / after clean	before	before	after	after
Juice flow rate at inlet ($m^3 \cdot h^{-1}$)	258.2	267.7	272.1	273.1
Calandria pressure (kPa abs)	62.3	64.1	47.9	47.4
Headspace pressure (kPa abs)	13.7	13.8	14.6	14.8
Condensate flow rate ($m^3 \cdot h^{-1}$)	136.3	135.6	141.6	138.2
Dynamic head (mm)	300	300	310	310
Juice temperature at inlet (°C)	87.8	88.9	81.3	81.3
Juice brix at inlet (%-wt)	35.6	36.3	37.7	38.1

Table 3.12 Summary of data used as boundary conditions for the CFD model of the Farleigh #2 vessel

Test no.	**1**	**2**	**3**	**4**	**5**	**6**
Before / after clean	before	before	before	before	after	after
Juice flow rate at inlet ($m^3 \cdot h^{-1}$)	365.3	315.3	262.8	277.7	344.9	341.0
Calandria pressure (kPa abs)	125.9	125.5	103.2	106.8	111.7	111.8
Headspace pressure (kPa abs)	98.0	97.7	81.7	82.6	87.4	88.3
Condensate flow rate ($m^3 \cdot h^{-1}$)	56.6	57.1	36.8	36.1	50.6	51.3
Dynamic head (mm)	571	530	443	450	424	440
Juice temperature at inlet (°C)	100.8	100.9	100.4	99.8	95.2	101.0
Juice brix at inlet (%-wt)	22.5	21.7	23.9	22.7	22.1	22.4

Table 3.13 and Table 3.14 provide a summary of the data points used for comparison with the CFD model predictions of the Proserpine #4 and the Farleigh #2 vessels respectively.

Table 3.13 Summary of data used for comparison with the CFD model of the Proserpine #4 vessel

Test no.	**1**	**2**	**3**	**4**
Juice temperature at point A (°C)	55.1	55.5	57.6	58.0
Juice temperature at point B (°C)	55.0	55.1	56.0	57.3
Juice temperature at point C (°C)	57.0	57.3	58.8	58.8
Juice brix at outlet (%-wt)	63.1	63.7	67.5	67.1
Juice brix at point A (%-wt)	63.5	64.4	68.5	68.1
Juice brix at point B (%-wt)	65.0	65.7	72.9	69.1
Juice brix at point C (%-wt)	63.6	64.5	67.1	66.7

Table 3.14 Summary of data used for comparison with the CFD model of the Farleigh #2 vessel

Test no.	1	2	3	4	5	6
Juice temperature at outlet#3a (°C)	99.3	99.3	93.2	94.5	n/a	n/a
Juice temperature at outlet#3b (°C)	99.0	99.3	92.1	93.3	92.6	93.7
Juice temperature at point A (°C)	98.4	98.5	91.9	93.3	92.2	95.2
Juice temperature at point B (°C)	97.3	97.2	91.3	92.6	92.4	94.0
Juice temperature at point C (°C)	n/a	95.0	90.2	92.3	93.1	94.7
Juice brix at outlet#3a (%-wt)	26.3	25.4	27.8	27.0	25.9	26.3
Juice brix at outlet#3b (%-wt)	26.8	25.9	28.2	27.2	26.6	26.9
Juice brix at point A (%-wt)	28.3	27.1	n/a	n/a	n/a	n/a
Juice brix at point B (%-wt)	27.4	26.4	28.7	27.5	26.9	27.2
Juice brix at point C (%-wt)	n/a	n/a	27.5	26.4	26.0	26.4

3.10 Summary of factory experiments

The accuracy of any CFD model must be determined prior to the model's application as an engineering design tool. The level of confidence in the predictions depends largely on the quality of the data used for comparison purposes. Prior to these experiments no factory data existed that is suitable for comparison with CFD model predictions of a sugar mill evaporator. In total, 10 tests were conducted on the two vessels under the widest possible range of operating conditions by conducting some tests immediately before and some immediately after the vessel was cleaned.

The heat and mass balance calculations performed on the data show conservation of heat and mass therefore, the associated brix and temperature distributions are considered to be suitably accurate. The data gathered as part of these experiments do not completely describe the brix and temperature distributions within the flow field, but they do provide a description in those areas where the largest juice brix and temperature gradients were expected (i.e. in the flow path from inlet towards the outlet). The results collated after the completion of the experiments do not show the expected steady increase in juice brix and temperature. However, since the locations of the tapping points are fixed, maximum use of the experimental results was made whilst recognising the limitations of the available data.